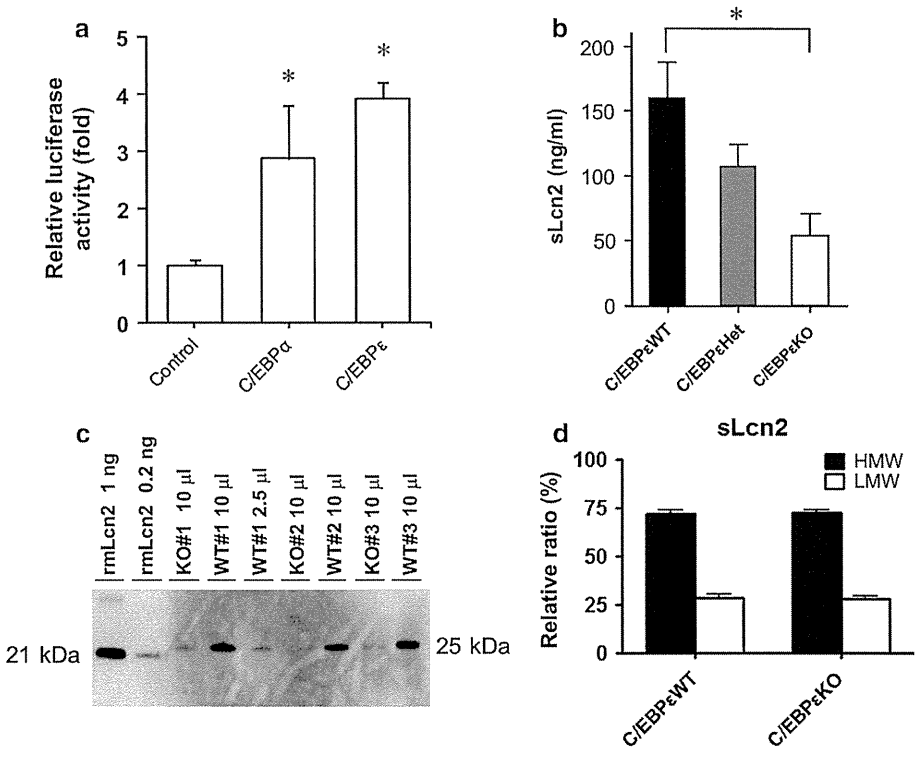

Fig. 5 C/EBPε-dependent LCN2 expression. **a** Effects of C/EBPα and ε overexpression upon human LCN2 promoter activity. Values are mean ± SEM. $n = 4$. $^*p < 0.05$ vs. control. **b** Serum total LCN2 levels including both HMW and LMW forms were measured by ELISA in C/EBPε knockout (KO), heterozygous (Het) and WT (wild-type) mice. $n = 4$. **c** Western blot analysis of serum LMW LCN2 from C/EBPε KO and WT mice (#1–3, respectively, $n = 3$). Serum aliquots (2.5 or 10 μl) from YM-100 flow through were separated by SDS-PAGE in reducing conditions. rmLCN2, recombinant mouse LCN2 as standards. **d** Relative ratios of high and low molecular weight LCN2 in the serum of C/EBPε KO and WT mice. $n = 4$

luciferase assay, overexpression of C/EBPε, as well as C/EBPα, significantly enhanced the promoter activity of LCN2 gene (Fig. 5a). Since C/EBPε$^{-/-}$ mice have severely impaired terminal differentiation of neutrophils [18, 22], these mice were utilized to determine the impact of C/EBPε-dependent neutrophil maturation on steady-state serum LCN2 levels. By ELISA, serum LCN2 levels in C/EBPε$^{-/-}$ and C/EBPε$^{+/-}$ mice were reduced by 66 ± 11 % ($p < 0.05$) and by 34 ± 12 %, respectively, as compared to C/EBPε$^{+/+}$ animals (Fig. 5b). Similar differences among genotypes were observed by Western blot of LMW (<100 kDa) fraction of the serum (Fig. 5c). These findings indicate that C/EBPε is essential for maintaining steady-state serum LCN2 levels in mice. As to molecular forms, approximately 72 % of serum LCN2 was in HMW form, and the ratio was not altered by absence of neutrophils in KO mice (Fig. 5d).

Discussion

Here, we have shown that serum LCN2 levels are decreased by 76 % during neutropenic conditions after SCT, consistently with our present findings in C/EBPε KO mice, which lack functionally mature neutrophils [18, 22]. Furthermore, serum LCN2 levels showed a strong correlation with blood neutrophil counts. These findings show, for the first time to our knowledge, that circulating neutrophils are the predominant source of steady-state blood LCN2.

LCN2 plays an essential role in host defense by inhibiting the growth of bacteria such as Escherichia coli and Mycobacterium tuberculosis [9, 23]. Therefore, not only neutropenia but also reduced circulating LCN2 levels may contribute to the high susceptibility of patients to infection during the neutrophil nadir periods after SCT. To date, it is not known whether subjects with supranormal circulating LCN2 levels are super-protected against infection.

When serum and urine LCN2 were separated into HMW and LMW forms, HMW LCN2 was the major form in blood, while urinary LCN2 consisted almost exclusively of LMW forms. These findings were quite surprising, since blood and urinary LCN2 levels are both elevated early in the course of AKI and both of these markers have been considered to be useful biomarkers of AKI [2, 6]. During nadir periods of the neutrophil counts, bacterial infection caused minimal elevation in serum LCN2 levels, but AKI lead to remarkable elevation in serum and urinary LCN2 levels. These findings suggest that the major source of serum LCN2 is the neutrophils in healthy and infected conditions, whereas the kidneys, especially the nephron segments of the thick ascending limbs of Henle and collecting ducts [2, 8, 11], are the main source of serum and urinary LCN2 in AKI. Cai et al. [24] examined molecular forms of LCN2 in the urine and reported that renal tubules mainly secrete monomer LCN2, whereas neutrophils

predominantly release dimer LCN2. Information concerning LCN2 in the blood was not provided in their work [24]. Of note, mature neutrophils contain large amount of LCN2 protein in the secretory granules but LCN2 mRNA expression is lost in these cells [1, 2, 25], making it very difficult to quantitatively evaluate neutrophil-derived LCN2 at the mRNA level. In patients with overt proteinuria (which suggests the presence of severe glomerular injury), HMW urinary LCN2 proteins were observed (Fig. 4b). At least some of HMW urinary LCN2 proteins are presumed to derive from the blood. Recently, we have been able to purify and identify several LCN2-binding proteins in the urine from patients with chronic kidney disease [26].

How is LCN2 synthesized in the kidney secreted in the blood or excreted in the urine deserves to be discussed. When we stained LCN2 protein in injured mouse kidneys in a previous study, we found 2 staining patterns [11]. One was a granular pattern along apical side of proximal tubules, which appears to reflect blood-driven, reabsorbed LCN2 protein. The other was diffusely distributed in the cytoplasm of distal nephron cells, and we speculate that LCN2 protein in this compartment is released into the urine or circulation, at least partially, through a non-specific pathway, not depending upon secretory granules. Indeed, wild-type kidney transplanted into LCN2 KO mice does release LCN2 protein in the urine (potentially through circulation) after induction of ischemic kidney injury [8].

A portion (15 %) of LCN2 in neutrophil secretory granules co-localizes with gelatinase B [3] and forms heterodimer with gelatinase B [1], preserving gelatinase B from degradation [27]. When we examined the concentration of LCN2/gelatinase B complex in the total LCN2 immunoreactivities in the blood of healthy subjects and patients undergoing SCT, the complex occupied <30 %. We also found that the ratio of the complex is largely reduced during neutropenic periods. These findings suggest that neutrophils are an important source of LCN2/gelatinase B complex in the blood but the complex only constitutes a small fraction of circulating LCN2.

There are several limitations in this study. The present study was mainly focused to longitudinal analysis of patients undergoing SCT, and the numbers of patients with hematologic or renal disorders and healthy subjects were small. Since severity of bacterial infection is generally larger when it is associated with AKI, higher peak serum and urinary LCN2 levels in Group 4 [bacterial infection (+), AKI (+)] compared to Group 2 [bacterial infection (+), AKI (−)] may have been caused not only by complicating AKI but also by more severe infection.

In conclusion, neutrophils are the predominant source of circulating LCN2 in physiological conditions, which may play an important role in the prevention of bacterial infection. In AKI, serum LCN2 proteins are dramatically increased even among patients in neutropenic states, suggesting that injured kidneys are major source of circulating LCN2 in pathologic conditions. The present study brings new insights into our understanding of the complicated regulation and clinical implication of blood or urinary LCN2 concentrations as biomarkers of AKI.

Acknowledgments The authors are grateful to Drs. K. Xanthopolous (Aurora Biosciences, San Diego, CA) and J. Lekstrom-Himes (the National Institutes of Health, Bethesda, MD) for providing C/EBPε knockout mice. C/EBP α cDNA was a kind gift from Dr. D.G. Tenen (Beth Israel Deaconess Medical Center and Harvard Medical School, Boston, MA). We also want to thank Ms. M. Nakaya (Abbott Japan, Matsudo, Japan) for discussion. This work was supported by grants from the Ministry of Education, Science, Sports and Culture of Japan (K.M., H.K. and M.M.), the Japan Kidney Foundation (K.M.), the Project Research from the High-Technology Center of Kanazawa Medical University (H.K.), the Smoking Research Foundation (M.M.), and the National Institutes of Health and A*STAR of Singapore (H.P.K.).

Conflict of interest K.M. and J.B. are a part of patent co-inventors for LCN2 as a diagnostic marker of renal failure. The other authors have no conflicts of interest to declare.

References

1. Kjeldsen L, Johnsen AH, Sengelov H, Borregaard N. Isolation and primary structure of NGAL, a novel protein associated with human neutrophil gelatinase. J Biol Chem. 1993;268:10425–32.
2. Mori K, Nakao K. Neutrophil gelatinase-associated lipocalin as the real-time indicator of active kidney damage. Kidney Int. 2007;71:967–70.
3. Cowland JB, Borregaard N. The individual regulation of granule protein mRNA levels during neutrophil maturation explains the heterogeneity of neutrophil granules. J Leukoc Biol. 1999;66:989–95.
4. Cowland JB, Borregaard N. Molecular characterization and pattern of tissue expression of the gene for neutrophil gelatinase-associated lipocalin from humans. Genomics. 1997;45:17–23.
5. Mori K, Lee HT, Rapoport D, Drexler IR, Foster K, Yang J, Schmidt-Ott KM, Chen X, Li JY, Weiss S, Mishra J, Cheema FH, Markowitz G, Suganami T, Sawai K, Mukoyama M, Kunis C, D'Agati V, Devarajan P, Barasch J. Endocytic delivery of lipocalin-siderophore-iron complex rescues the kidney from ischemia-reperfusion injury. J Clin Invest. 2005;115:610–21.
6. Mishra J, Dent C, Tarabishi R, Mitsnefes MM, Ma Q, Kelly C, Ruff SM, Zahedi K, Shao M, Bean J, Mori K, Barasch J, Devarajan P. Neutrophil gelatinase-associated lipocalin (NGAL) as a biomarker for acute renal injury after cardiac surgery. Lancet. 2005;365:1231–8.
7. Nickolas TL, O'Rourke MJ, Yang J, Sise ME, Canetta PA, Barasch N, Buchen C, Khan F, Mori K, Giglio J, Devarajan P, Barasch J. Sensitivity and specificity of a single emergency department measurement of urinary neutrophil gelatinase-associated lipocalin for diagnosing acute kidney injury. Ann Intern Med. 2008;148:810–9.
8. Paragas N, Qiu A, Zhang Q, Samstein B, Deng SX, Schmidt-Ott KM, Viltard M, Yu W, Forster CS, Gong G, Liu Y, Kulkarni R,

Mori K, Kalandadze A, Ratner AJ, Devarajan P, Landry DW, D'Agati V, Lin CS, Barasch J. The NGAL reporter mouse detects the response of the kidney to injury in real time. Nat Med. 2011;17:216–22.
9. Flo TH, Smith KD, Sato S, Rodriguez DJ, Holmes MA, Strong RK, Akira S, Aderem A. Lipocalin 2 mediates an innate immune response to bacterial infection by sequestrating iron. Nature. 2004;432:917–21.
10. Yang J, Goetz D, Li JY, Wang W, Mori K, Setlik D, Du T, Erdjument-Bromage H, Tempst P, Strong R, Barasch J. An iron delivery pathway mediated by a lipocalin. Mol Cell. 2002;10: 1045–56.
11. Kuwabara T, Mori K, Mukoyama M, Kasahara M, Yokoi H, Saito Y, Yoshioka T, Ogawa Y, Imamaki H, Kusakabe T, Ebihara K, Omata M, Satoh N, Sugawara A, Barasch J, Nakao K. Urinary neutrophil gelatinase-associated lipocalin levels reflect damage to glomeruli, proximal tubules, and distal nephrons. Kidney Int. 2009;75:285–94.
12. Bolignano D, Lacquaniti A, Coppolino G, Donato V, Campo S, Fazio MR, Nicocia G, Buemi M. Neutrophil gelatinase-associated lipocalin (NGAL) and progression of chronic kidney disease. Clin J Am Soc Nephrol. 2009;4:337–44.
13. Xu SY, Pauksen K, Venge P. Serum measurements of human neutrophil lipocalin (HNL) discriminate between acute bacterial and viral infections. Scand J Clin Lab Invest. 1995;55:125–31.
14. Martensson J, Bell M, Oldner A, Xu S, Venge P, Martling CR. Neutrophil gelatinase-associated lipocalin in adult septic patients with and without acute kidney injury. Intensive Care Med. 2010;36:1333–40.
15. Kjeldsen L, Johnsen AH, Sengelov H, Borregaard N. Isolation and primary structure of NGAL, a novel protein associated with human neutrophil gelatinase. J Biol Chem. 1993;268:10425–32.
16. Rudd PM, Mattu TS, Masure S, Bratt T, Van den Steen PE, Wormald MR, Küster B, Harvey DJ, Borregaard N, Van Damme J, Dwek RA, Opdenakker G. Glycosylation of natural human neutrophil gelatinase B and neutrophil gelatinase B-associated lipocalin. Biochemistry. 1999;38:13937–50.
17. Kanda J, Mizumoto C, Kawabata H, Tsuchida H, Tomosugi N, Matsuo K, Uchiyama T. Serum hepcidin level and erythropoietic activity after hematopoietic stem cell transplantation. Haematologica. 2008;93:1550–4.
18. Yamanaka R, Barlow C, Lekstrom-Himes J, Castilla LH, Liu PP, Eckhaus M, Decker T, Wynshaw-Boris A, Xanthopoulos KG. Impaired granulopoiesis, myelodysplasia, and early lethality in CCAAT/enhancer binding protein epsilon-deficient mice. Proc Natl Acad Sci USA. 1997;94:13187–92.
19. Radomska HS, Huettner CS, Zhang P, Cheng T, Scadden DT, Tenen DG. CCAAT/enhancer binding protein alpha is a regulatory switch sufficient for induction of granulocytic development from bipotential myeloid progenitors. Mol Cell Biol. 1998; 18:4301–14.
20. Chumakov AM, Grillier I, Chumakova E, Chih D, Slater J, Koeffler HP. Cloning of the novel human myeloid-cell-specific C/EBP-epsilon transcription factor. Mol Cell Biol. 1997;17: 1375–86.
21. Axelsson L, Bergenfeldt M, Ohlsson K. Studies of the release and turnover of a human neutrophil lipocalin. Scand J Clin Lab Invest. 1995;55:577–88.
22. Gombart AF, Kwok SH, Anderson KL, Yamaguchi Y, Torbett BE, Koeffler HP. Regulation of neutrophil and eosinophil secondary granule gene expression by transcription factors C/EBP epsilon and PU.1. Blood. 2003;101:3265–73.
23. Saiga H, Nishimura J, Kuwata H, Okuyama M, Matsumoto S, Sato S, Matsumoto M, Akira S, Yoshikai Y, Honda K, Yamamoto M, Takeda K. Lipocalin 2-dependent inhibition of mycobacterial growth in alveolar epithelium. J Immunol. 2008;181:8521–7.
24. Cai L, Rubin J, Han W, Venge P, Xu S. The origin of multiple molecular forms in urine of HNL/NGAL. Clin J Am Soc Nephrol. 2010;5:2229–35.
25. Cowland JB, Borregaard N. The individual regulation of granule protein mRNA levels during neutrophil maturation explains the heterogeneity of neutrophil granules. J Leukoc Biol. 1999;66: 989–95.
26. Nickolas TL, Forster CS, Sise ME, Barasch N, Valle DS, Viltard M, Buchen C, Kupferman S, Carnevali ML, Bennett M, Mattei S, Bovino A, Argentiero L, Magnano A, Devarajan P, Mori K, Erdjument-Bromage H, Tempst P, Allegri L, Barasch J. NGAL (LCN2) monomer is associated with tubulointerstitial damage in chronic kidney disease. Kidney Int. 2012;82:718–22
27. Yan L, Borregaard N, Kjeldsen L, Moses MA. The high molecular weight urinary matrix metalloproteinase (MMP) activity is a complex of gelatinase B/MMP-9 and neutrophil gelatinase-associated lipocalin (NGAL). Modulation of MMP-9 activity by NGAL. J Biol Chem. 2001;276:37258–65.

frontiers in
ENDOCRINOLOGY

MINI REVIEW ARTICLE
published: 26 September 2014
doi: 10.3389/fendo.2014.00152

The G-protein-coupled long-chain fatty acid receptor GPR40 and glucose metabolism

Tsutomu Tomita[1]*, Kiminori Hosoda[1], Junji Fujikura[1], Nobuya Inagaki[1] and Kazuwa Nakao[2]

[1] Department of Diabetes, Endocrinology and Nutrition, Kyoto University Graduate School of Medicine, Kyoto, Japan
[2] Medical Innovation Center, Kyoto University Graduate School of Medicine, Kyoto, Japan

Edited by:
Ikuo Kimura, Tokyo University of Agriculture and Technology, Japan

Reviewed by:
Carol Huang, University of Calgary, Canada
Kay Waud, Jones Institute for Reproductive Medicine, USA

***Correspondence:**
Tsutomu Tomita, Department of Diabetes, Endocrinology and Nutrition, Kyoto University Graduate School of Medicine, 54 Shogoin Kawaharacho, Sakyo, Kyoto 606-8507, Japan
e-mail: tt@kuhp.kyoto-u.ac.jp

Free fatty acids (FFAs) play a pivotal role in metabolic control and cell signaling processes in various tissues. In particular, FFAs are known to augment glucose-stimulated insulin secretion by pancreatic beta cells, where fatty acid-derived metabolites, such as long-chain fatty acyl-CoAs, are believed to act as crucial effectors. Recently, G-protein-coupled receptor 40 (GPR40), a receptor for long-chain fatty acids, was reported to be highly expressed in pancreatic beta cells and involved in the regulation of insulin secretion. Hence, GPR40 is considered to be a potential therapeutic target for the treatment of diabetes. In this review, we summarize the identification and gene expression patterns of GPR40 and its role in glucose metabolism. We also discuss the potential application of GPR40 as a therapeutic target.

Keywords: GPR40, FFAR1, LCFA, insulin secretion, pancreatic beta cells

INTRODUCTION

Free fatty acids (FFAs) are essential nutrients that also act as signaling molecules in various tissues. Long-chain fatty acids (LCFAs) play a role in the augmentation of glucose-stimulated insulin secretion (GSIS) (1). GSIS was observed to be considerably decreased by FFA depletion following *in vivo* administration of nicotinic acid to rats (2) and humans (3). Thus, FFA-mediated augmentation is considered to be physiologically significant. However, the underlying mechanisms of FFA-mediated augmentation of GSIS have not been fully elucidated. Several investigators have recently demonstrated that FFAs act as ligands for membrane-bound G-protein-coupled receptors (GPCRs) such as G-protein-coupled receptor 40 (GPR40), GPR41, GPR43, and GPR120. Among these, GPR40 is preferentially expressed by pancreatic beta cells in rodents and augments GSIS after acute exposure to LCFAs, highlighting the role of GPR40 as a potential key molecule in the regulation of insulin secretion.

LCFA RECEPTOR GPR40

GPR40 consists of 300 residues and was originally reported as an orphan GPCR (4). GPR40 was deorphaned by screening using a fluorometric imaging plate reader (FLIPR) system, which detects increases in Ca^{2+} concentrations in cultured cells with transiently expressed GPR40 cDNA (5, 6). GPR40 is reportedly activated by LCFAs (C12–22) and several eicosanoids in theoretically physiological concentration ranges. The profiles of putative GPR40 ligands are well conserved among mice, rats, and humans (5).

GPR40 GENE EXPRESSION IN RODENTS

Among rat tissues, GPR40 mRNA is almost exclusively expressed in the pancreas. In pancreatic islets, GPR40 mRNA levels were found to be approximately 17-fold higher than the levels in the pancreas, suggesting selective GPR40 expression by pancreatic islets. Considerable amounts of GPR40 mRNA were detected in the pancreatic beta cell lines MIN6, betaTC-3, HIT-T15, and Rin5F but not in the pancreatic alpha cell line alphaTC1. Furthermore, *in situ* hybridization with rat pancreatic islets suggested that GPR40 mRNA is preferentially expressed in pancreatic beta cells (5).

Reports using anti-GPR40 antibodies suggest that GPR40 protein is also probably preferentially expressed in pancreatic islets (7, 8).

ROLES OF GPR40 IN REGULATION OF INSULIN SECRETION

In MIN6 cells, insulin secretion was augmented by LCFAs in a dose-dependent manner, and the augmentation was observed only under hyperglycemic conditions (11–22 mM) (5), indicating the LCFA-mediated augmentation of insulin secretion is glucose-dependent. Silencing of GPR40 gene expression using siRNA almost abolished the augmentation effects of LCFAs, indicating that GPR40 is involved in LCFA-mediated regulation of insulin secretion. GPR40 is a class A GPCR, highlighting the potential of GPR40 as a target for novel anti-diabetic oral drugs with low risk of hypoglycemia, considering that LCFA-mediated augmentation of insulin secretion is glucose-dependent.

GPR40 GENE EXPRESSION IN HUMANS

Although GPR40 is reportedly preferentially expressed by pancreatic beta cells in both rats and mice, little is known about GPR40 gene expression in humans. In this context, we assessed GPR40 mRNA expression in fresh human tissues obtained during surgery (9, 10). Analysis of 12 specimens of non-tumor pancreatic tissues revealed a considerable amount of GPR40 mRNA in each. In three pancreatic islet tissues specimens, GPR40 mRNA levels were approximately 20-fold higher than those in pancreatic tissues, comparable to the levels of sulfonylurea receptor 1, which is

known to be highly expressed in pancreatic beta cells. High levels of GPR40 mRNA were detected in insulinoma (beta cell tumor) tissues in three cases; in contrast, GPR40 mRNA was undetectable in glucagonoma (alpha cell tumor) tissues (10, 11). In human pancreas, GPR40 mRNA level is positively and significantly correlated with the insulinogenic index, an index reflecting the function of pancreatic beta cells. These results indicate that GPR40 is highly expressed in human pancreatic beta cells and possibly involved in the positive regulation of insulin secretion (10).

REGULATION OF GPR40 GENE EXPRESSION

Though the mechanisms underlying the regulation of GPR40 gene expression is not fully understood, possible mechanisms include the PDX-1/IPF1 (12), which reportedly binds to the promoter region of the GPR40 gene (13). Moreover, nutrients and therapeutic drugs such as glucose (12), palmitate, and rosiglitazone (8) are reportedly involved in the regulation of GPR40 gene expressions.

THERAPEUTIC IMPLICATIONS OF GPR40

Although an initial report of systemic GPR40 knockout (KO) mice and beta cell-specific GPR40 transgenic (Tg) mice using the PDX-1/IPF1 promoter suggested possible involvement of GPR40 in insulin resistance in the liver and beta cell failure (14), later reports using GPR40 KO mice found no link between GPR40 and beta cell dysfunction (15, 16). Studies using GPR40 KO mice suggest the implication of GPR40 in the regulation of insulin secretion, at least under some conditions including loading of intralipid (17), high-fat diet (15), hyperglycemic glucose clamp, and arginine (18). Furthermore, GPR40 Tg mice with the mouse INS2 promoter exhibited better glucose tolerance with enhanced GSIS (19), suggesting therapeutic implications of GPR40 rather than a gateway of beta cell toxicity.

Additionally, recent reports suggest that GPR40 is expressed in enteroendocrine cells and involved in the positive regulation of intestinal hormones including glucagon-like peptide-1 (GLP-1), glucose-dependent insulinotropic polypeptide (GIP), and cholecystokinin (20–22).

GPR40 AGONISTS AS ANTI-DIABETIC DRUGS

Recently, TAK-875 (Fasiglifam), a novel GPR40 selective agonist (23), was reported as a potential oral anti-diabetic drug. The potency of TAK-875 is approximately 400-fold greater than that of the endogenous ligand oleic acid (24), and it does not activate GPR120 (23), another GPCR for LCFAs. TAK-875 augmented insulin secretion under high-glucose conditions in the rat pancreatic beta cell line INS1 833/14 (24) and human pancreatic islets (25) but did not affect glucagon secretion in humans (25), in accordance with the observations in humans by our group and others (9–11). TAK-875 significantly improved glycemic control with the augmentation of insulin secretion in diabetic rat models such as Wistar fatty rats (23) and Zucker diabetic fatty rats (24).

In phase 2, randomized, double-blind, placebo-controlled trial in patients with type 2 diabetes, HbA1c was decreased in a dose-dependent manner in TAK-875 groups, and the HbA1c-lowering effect (50–200 mg, approximately −1.1% in 12 weeks) was comparable to that in glimepiride (4 mg) group, while the incidence of hypoglycemia in TAK-875 was similar to the placebo group and markedly lower than the glimepiride group (26). In Japanese patients with type 2 diabetes, 12-week treatment with TAK-875 also decreased HbA1c levels in a dose-dependent manner, and the HbA1c-lowering effect (50–200 mg, approximately −1.3%) was comparable to that in the glimepiride (1 mg) group (27).

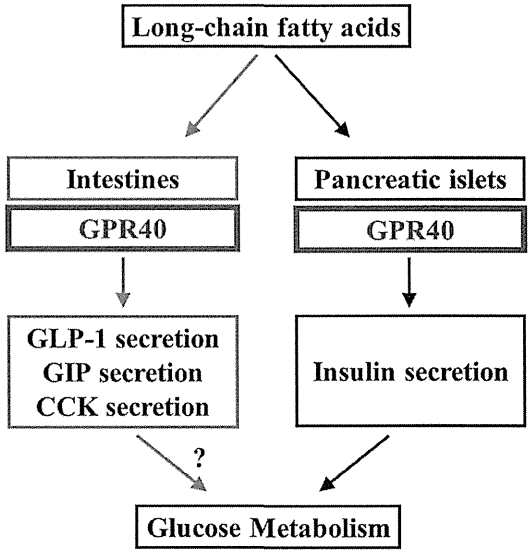

FIGURE 1 | LCFAs augment insulin secretion by stimulating GPR40 in beta cells in the pancreas. GPR40 is also reportedly involved in the positive regulation of secretion of some intestinal hormones. Studies using GPR40 agonists and analyses of beta cell-specific GPR40 transgenic mice indicate that GPR40 is involved in the regulation of glucose metabolism, at least by the augmentation of insulin secretion. Because LCFA-mediated augmentation of insulin secretion is glucose-dependent, GPR40 is thought to be a potential target for novel anti-diabetic drugs with low risk of hypoglycemia.

Though TAK-875 seemed to be a promising anti-diabetic drug, regrettably, its development was terminated in 2013 because of the risk of possible liver damage. Although the cause of the liver damage remains unclear, GPR40 is not expressed in the human liver (6, 10), suggesting that the toxicity may not be due to the GPR40 receptor itself but chemical characteristic of TAK-875 or its dose used in the clinical trials. Still, several GPR40 agonists continue to be evaluated in both preclinical (Bristol-Myers Squibb, Merck, Amgen, Johnson & Johnson, Astellas, Daiichi Sankyo, Piramal, and Connexios) and clinical (Japan Tobacco) trials, and the further development is expected in the study elucidating the significance of GPR40 in glucose and other metabolism.

CONCLUSION

Incretin mimetic-type drugs have been implicated in GPCR-mediated regulation of insulin secretion in diabetes. GPR40 is a GPCR that is highly expressed in pancreatic beta cells and involved in insulin secretion in rodents and humans. Hence, GPR40 is a potential therapeutic target in diabetes, which can lead to the development of oral drugs with fewer hypoglycemic side effects. Furthermore, GPR40 is reportedly implicated in the regulation of incretin secretion from enteroendocrine cells. GPR40 may be important to unveil the link between FFA signaling and beta

cell function as well as glucose metabolism (**Figure 1**). Hence, further studies are warranted to elucidate the physiological and pathophysiological implications of GPR40.

REFERENCES

1. Stein DT, Esser V, Stevenson BE, Lane KE, Whiteside JH, Daniels MB, et al. Essentiality of circulating fatty acids for glucose-stimulated insulin secretion in the fasted rat. *J Clin Invest* (1996) **97**:2728–35. doi:10.1172/JCI118727
2. Dobbins RL, Chester MW, Stevenson BE, Daniels MB, Stein DT, McGarry JD. A fatty acid-dependent step is critically important for both glucose- and non-glucose-stimulated insulin secretion. *J Clin Invest* (1998) **101**:2370–6. doi:10.1172/JCI1813
3. Dobbins RL, Chester MW, Daniels MB, McGarry JD, Stein DT. Circulating fatty acids are essential for efficient glucose-stimulated insulin secretion after prolonged fasting in humans. *Diabetes* (1998) **47**:1613–8. doi:10.2337/diabetes.47.10.1613
4. Takeda S, Kadowaki S, Haga T, Takaesu H, Mitaku S. Identification of G protein-coupled receptor genes from the human genome sequence. *FEBS Lett* (2002) **520**:97–101. doi:10.1016/S0014-5793(02)02775-8
5. Itoh Y, Kawamata Y, Harada M, Kobayashi M, Fujii R, Fukusumi S, et al. Free fatty acids regulate insulin secretion from pancreatic beta cells through GPR40. *Nature* (2003) **422**:173–6. doi:10.1038/nature01478
6. Briscoe CP, Tadayyon M, Andrews JL, Benson WG, Chambers JK, Eilert MM, et al. The orphan G protein-coupled receptor GPR40 is activated by medium and long chain fatty acids. *J Biol Chem* (2003) **278**:11303–11. doi:10.1074/jbc.M211495200
7. Hirasawa A, Itsubo C, Sadakane K, Hara T, Shinagawa S, Koga H, et al. Production and characterization of a monoclonal antibody against GPR40 (FFAR1; free fatty acid receptor 1). *Biochem Biophys Res Commun* (2008) **365**:22–8. doi:10.1016/j.bbrc.2007.10.142
8. Meidute Abaraviciene S, Muhammed SJ, Amisten S, Lundquist I, Salehi A. GPR40 protein levels are crucial to the regulation of stimulated hormone secretion in pancreatic islets. Lessons from spontaneous obesity-prone and non-obese type 2 diabetes in rats. *Mol Cell Endocrinol* (2013) **381**:150–9. doi:10.1016/j.mce.2013.07.025
9. Tomita T, Masuzaki H, Noguchi M, Iwakura H, Fujikura J, Tanaka T, et al. GPR40 gene expression in human pancreas and insulinoma. *Biochem Biophys Res Commun* (2005) **338**:1788–90. doi:10.1016/j.bbrc.2005.10.161
10. Tomita T, Masuzaki H, Iwakura H, Fujikura J, Noguchi M, Tanaka T, et al. Expression of the gene for a membrane-bound fatty acid receptor in the pancreas and islet cell tumours in humans: evidence for GPR40 expression in pancreatic beta cells and implications for insulin secretion. *Diabetologia* (2006) **49**:962–8. doi:10.1007/s00125-006-0193-8
11. Odori S, Hosoda K, Tomita T, Fujikura J, Kusakabe T, Kawaguchi Y, et al. GPR119 expression in normal human tissues and islet cell tumors: evidence for its islet-gastrointestinal distribution, expression in pancreatic beta and alpha cells, and involvement in islet function. *Metabolism* (2013) **62**:70–8. doi:10.1016/j.metabol.2012.06.010
12. Kebede M, Ferdaoussi M, Mancini A, Alquier T, Kulkarni RN, Walker MD, et al. Glucose activates free fatty acid receptor 1 gene transcription via phosphatidylinositol-3-kinase-dependent O-GlcNAcylation of pancreas-duodenum homeobox-1. *Proc Natl Acad Sci U S A* (2012) **109**:2376–81. doi:10.1073/pnas.1114350109
13. Bartoov-Shifman R, Ridner G, Bahar K, Rubins N, Walker MD. Regulation of the gene encoding GPR40, a fatty acid receptor expressed selectively in pancreatic beta cells. *J Biol Chem* (2007) **282**:23561–71. doi:10.1074/jbc.M702115200
14. Steneberg P, Rubins N, Bartoov-Shifman R, Walker MD, Edlund H. The FFA receptor GPR40 links hyperinsulinemia, hepatic steatosis, and impaired glucose homeostasis in mouse. *Cell Metab* (2005) **1**:245–58. doi:10.1016/j.cmet.2005.03.007
15. Kebede M, Alquier T, Latour MG, Semache M, Tremblay C, Poitout V. The fatty acid receptor GPR40 plays a role in insulin secretion in vivo after high-fat feeding. *Diabetes* (2008) **57**:2432–7. doi:10.2337/db08-0553
16. Lan H, Hoos LM, Liu L, Tetzloff G, Hu W, Abbondanzo SJ, et al. Lack of FFAR1/GPR40 does not protect mice from high-fat diet-induced metabolic disease. *Diabetes* (2008) **57**:2999–3006. doi:10.2337/db08-0596
17. Latour MG, Alquier T, Oseid E, Tremblay C, Jetton TL, Luo J, et al. GPR40 is necessary but not sufficient for fatty acid stimulation of insulin secretion in vivo. *Diabetes* (2007) **56**:1087–94. doi:10.2337/db06-1532
18. Alquier T, Peyot ML, Latour MG, Kebede M, Sorensen CM, Gesta S, et al. Deletion of GPR40 impairs glucose-induced insulin secretion in vivo in mice without affecting intracellular fuel metabolism in islets. *Diabetes* (2009) **58**:2607–15. doi:10.2337/db09-0362
19. Nagasumi K, Esaki R, Iwachidow K, Yasuhara Y, Ogi K, Tanaka H, et al. Overexpression of gpr40 in pancreatic β-cells augments glucose stimulated insulin secretion and improves glucose tolerance in normal and diabetic mice. *Diabetes* (2009) **58**:1067–76. doi:10.2337/db08-1233
20. Edfalk S, Steneberg P, Edlund H. Gpr40 is expressed in enteroendocrine cells and mediates free fatty acid stimulation of incretin secretion. *Diabetes* (2008) **57**:2280–7. doi:10.2337/db08-0307
21. Parker HE, Habib AM, Rogers GJ, Gribble FM, Reimann F. Nutrient-dependent secretion of glucose-dependent insulinotropic polypeptide from primary murine K cells. *Diabetologia* (2009) **52**:289–98. doi:10.1007/s00125-008-1202-x
22. Liou AP, Lu X, Sei Y, Zhao X, Pechhold S, Carrero RJ, et al. The G-protein-coupled receptor GPR40 directly mediates long-chain fatty acid-induced secretion of cholecystokinin. *Gastroenterology* (2011) **140**:903–12. doi:10.1053/j.gastro.2010.10.012
23. Negoro N, Sasaki S, Mikami S, Ito M, Suzuki M, Tsujihata Y, et al. Discovery of TAK-875: a potent, selective, and orally bioavailable GPR40 agonist. *ACS Med Chem Lett* (2010) **1**:290–4. doi:10.1021/ml1000855
24. Tsujihata Y, Ito R, Suzuki M, Harada A, Negoro N, Yasuma T, et al. TAK-875, an orally available G protein-coupled receptor 40/free fatty acid receptor 1 agonist, enhances glucose-dependent insulin secretion and improves both postprandial and fasting hyperglycemia in type 2 diabetic rats. *J Pharmacol Exp Ther* (2011) **339**:228–37. doi:10.1124/jpet.111.183772
25. Yashiro H, Tsujihata Y, Takeuchi K, Hazama M, Johnson PR, Rorsman P. The effects of TAK-875, a selective G protein-coupled receptor 40/free fatty acid 1 agonist, on insulin and glucagon secretion in isolated rat and human islets. *J Pharmacol Exp Ther* (2012) **340**:483–9. doi:10.1124/jpet.111.187708
26. Burant CF, Viswanathan P, Marcinak J, Cao C, Vakilynejad M, Xie B, et al. TAK-875 versus placebo or glimepiride in type 2 diabetes mellitus: a phase 2, randomised, double-blind, placebo-controlled trial. *Lancet* (2012) **379**:1403–11. doi:10.1016/S0140-6736(11)61879-5
27. Kaku K, Araki T, Yoshinaka R. Randomized, double-blind, dose-ranging study of TAK-875, a novel GPR40 agonist, in Japanese patients with inadequately controlled type 2 diabetes. *Diabetes Care* (2013) **36**:245–50. doi:10.2337/dc12-0872

Conflict of Interest Statement: The authors declare that the research was conducted in the absence of any commercial or financial relationships that could be construed as a potential conflict of interest.

Received: 12 June 2014; accepted: 12 September 2014; published online: 26 September 2014.

Citation: Tomita T, Hosoda K, Fujikura J, Inagaki N and Nakao K (2014) The G-protein-coupled long-chain fatty acid receptor GPR40 and glucose metabolism. Front. Endocrinol. 5:152. doi: 10.3389/fendo.2014.00152

This article was submitted to Diabetes, a section of the journal Frontiers in Endocrinology.

OXFORD

Human Molecular Genetics, 2015, 1–12

doi: 10.1093/hmg/ddv156
Advance Access Publication Date: 1 May 2015
Original Article

ORIGINAL ARTICLE

Seipin is necessary for normal brain development and spermatogenesis in addition to adipogenesis

Chihiro Ebihara[1], Ken Ebihara[1,5,*], Megumi Aizawa-Abe[1,5], Tomoji Mashimo[2], Tsutomu Tomita[1], Mingming Zhao[1], Valentino Gumbilai[1], Toru Kusakabe[1,3], Yuji Yamamoto[1], Daisuke Aotani[1,3], Sachiko Yamamoto-Kataoka[1], Takeru Sakai[1], Kiminori Hosoda[1,5,4], Tadao Serikawa[2] and Kazuwa Nakao[1,3]

[1]Department of Medicine and Clinical Science, [2]Institute of Laboratory Animals, [3]Medical Innovation Center, [4]Department of Health and Science, Kyoto University Graduate School of Medicine, Kyoto 6068507, Japan and [5]Institute for Advancement of Clinical and Translational Science, Kyoto University Hospital, Kyoto, Japan

*To whom correspondence should be addressed at: Division of Endocrinology and Metabolism, Jichi Medical University, Tochigi 3290433, Japan. Tel: +81 285587355; Fax: +81 285448143; Email: kebihara@jichi.ac.jp

Abstract

Seipin, encoded by *BSCL2* gene, is a protein whose physiological functions remain unclear. Mutations of *BSCL2* cause the most-severe form of congenital generalized lipodystrophy (CGL). *BSCL2* mRNA is highly expressed in the brain and testis in addition to the adipose tissue in human, suggesting physiological roles of seipin in non-adipose tissues. Since we found *BSCL2* mRNA expression pattern among organs in rat is similar to human while it is not highly expressed in mouse brain, we generated a *Bscl2*/seipin knockout (SKO) rat using the method with ENU (*N*-ethyl-*N*-nitrosourea) mutagenesis. SKO rats showed total lack of white adipose tissues including mechanical fat such as bone marrow and retro-orbital fats, while physiologically functional brown adipose tissue was preserved. Besides the lipodystrophic phenotypes, SKO rats showed impairment of spatial working memory with brain weight reduction and infertility with azoospermia. We confirmed reduction of brain volume and number of sperm in human patients with *BSCL2* mutation. This is the first report demonstrating that seipin is necessary for normal brain development and spermatogenesis in addition to white adipose tissue development.

Introduction

Seipin is a protein encoded by *BSCL2* gene whose mutation causes the most severe variety of congenital generalized lipodystrophy (CGL), also known as Berardinelli-Seip congenital lipodystrophy (BSCL) (1). BSCL is a disease characterized by a near total lack of adipose tissue from birth (2). Patients with BSCL frequently develop severe insulin resistance, hypertriglyceridemia and fatty liver (3). BSCL due to *AGPAT2* (BSCL1), *BSCL2* (BSCL2), *CAV1* (BSCL3) and *PTRF* (BSCL4) mutations have been reported so far (1,4–6). BSCL1 and BSCL 2 are the most common varieties and have been reported in patients of various ethnicities (3). However, most of the patients of African origin have *AGPAT2* mutation and those from Lebanon have *BSCL2* mutation. *BSCL2* mutation is also the major cause of BSCL in Japan (7).

1-acylglycerol-3-phosphate O-acyltransferase (AGPAT) is a critical enzymes involved in the biosynthesis of triglyceride and phospholipids from glycerol-3-phosphate. Of known AGPAT isoforms, AGPAT2 is highly expressed in the adipose tissue and its deficiency causes lipodystrophy (8). Caveolin 1 encoded by *CAV1* is an integral component of caveolae, which are specialized microdomains seen in abundance on adipocyte membranes (9). Caveolin 1 binds fatty acids and translocates them to lipid droplets. Polymerase 1 and transcript release factor (PTRF) is involved in biogenesis of caveolae and regulates expression of

Received: February 5, 2015. **Revised:** March 31, 2015. **Accepted:** April 27, 2015

caveolins 1and 3 (6). On the other hand, molecular functions of seipin, a protein encoded by *BSCL2* remain unclear although seipin seems to play a role in lipid droplet formation and be involved in adipocyte differentiation. While *BSCL2* mutations cause the most severe cases of BSCL, yet seipin remains the most mysterious lipodystrophic protein in terms of function.

Seipin is a 398 (short-form) or 462 (long-form) amino acid protein that has no similarity with other known proteins or consensus motif. Seipin has two distinct hydrophobic amino acid stretches and is speculated to have two transmembrane domains (1). It also has been shown that seipin localizes to endoplasmic reticulum in various cell lines (10–12). *BSCL2* mRNA is highly expressed in the brain and the testis other than adipose tissue in human (1). BSCL2 patients exhibit much higher rate of mild mental retardation than do other BSCL patients (13). These evidences strongly suggest physiological roles of seipin in non-adipose tissues.

In the past few years, three independent models of *Bscl2* knockout mice have been reported (14–16). All these three knockout mice exhibited severe generalized lipodystrophy, demonstrating clearly that seipin deficiency itself leads to generalized lipodystrophy *in vivo*. However, in contrast to human BSCL2 patients, all the three knockout mice had low plasma triglyceride levels. In addition, *Bscl2* knockout mice showed a decrease of energy expenditure that is generally increased in human BSCL2 patients (16,17). There are also some differences between mouse and human on physiological roles of seipin in non-adipose tissues. Although depression that is not a major symptom in human BSCL2 patients was reported in male *Bscl2* knockout mice (18), no phenotypes as to mental retardation that is frequently observed in human BSCL2 patients have been reported in *Bscl2* knockout mice. While *BSCL2* mRNA is highly expressed in the brain and testis in addition to the adipose tissue in human, *BSCL2* mRNA is not highly expressed in mouse brain (11). Furthermore, teratozoospermia was reported in *Bscl2* knockout mice (19) but was not observed in our male BSCL2 patients. Instead of that, oligospermia was observed in our BSCL2 patients. Thus, a new animal model of human BSCL2 is required for further understanding of physiological roles of seipin.

In this study, we chose rat as a species for the generation of a new animal model of human BSCL2 after confirming the similarity of *BSCL2* mRNA expression pattern between rat and human. We generated a *Bscl2*/seipin knockout (SKO) rat using with the *N*-ethyl-*N*-nitrosourea (ENU) mutagenesis method (20). SKO rat has a homozygous nonsense mutation (L20X) in *BSCL2* gene, which is upstream of the first transmembrane domain. SKO rats showed impairment of spatial working memory with reduction of whole brain weight and infertility with azoospermia in addition to phenotypes of lipodystrophy including hypertriglyceridemia and increase of energy expenditure. Therefore, we also analyzed brain volume and semen in human BSCL2 patients. This is the first report demonstrating that seipin is necessary for normal brain development and spermatogenesis in addition to white adipose tissue development.

Results

BSCL2 mRNA expression profiles in mouse and rat

It was reported that *BSCL2* mRNA is highly expressed in the brain and the testis in human (1). To choose an animal species that is appropriate for generating the experimental model of human BSCL2, we examined *Bscl2* mRNA expressions in various tissues in mouse and rat and compared these expression profiles with that in human. In mouse, high expression of *Bscl2* mRNA was observed in the testis but not in the brain (Fig. 1A). On the other hand, *Bscl2* mRNA was highly expressed in both the brain and the testis in rat like in human (Fig. 1B). Thus, we decided to generate a seipin knockout animal on rat background as a human BSCL2 model.

Generation of seipin knockout rat

By using ENU mutagenesis followed by MuT-POWER screening of the KURMA samples (20), we generated a seipin knockout rat with a homozygous nonsense mutation ($Bscl2^{sko/sko}$) in *Bscl2*, the seipin gene. $Bscl2^{sko}$ mutation was T to A transition at nucleotide 239 in the third exon of *Bscl2* gene, resulted in a substitution of leucine at codon 20 by the stop codon (L20X), which is upstream of the first transmembrane domain (Fig. 1C and D). Male and female heterozygous SKO rats were intercrossed to obtain homozygous SKO animals. There were 19 homozygous WT, 50 heterozygous SKO and 26 homozygous SKO rats. This ratio did not differ significantly from the expected 1:2:1 Mendelian ratio of genotypes (number of delivery = 10, mean number of pups per delivery = 9.5; $c^2 = 1.29$, $P = 0.69$). The sex ratios also did not differ significantly from the expected ratio (male; $n = 48$, female; $n = 45$; $c^2 = 0.58$, $P = 0.45$).

The body weight in SKO rats was significantly lower than that in their WT littermates from at least 3 weeks after birth (Fig. 1E). There was no difference of body weight between heterozygous SKO rats and their WT littermates (data not shown). Although there was no significant difference in the amount of food intake and respiratory exchange ratio, the oxygen consumption was significantly higher in SKO rats compared with their WT littermates (Supplementary Material, Fig. S1A–C). When weights of various tissues were compared between SKO and WT rats, the weight in most tissues was significantly increased in SKO rats (Fig. 1F), which might be the organomegaly caused by hyperinsulinemia. In contrast, in addition to the WAT and BAT, weights in the brain and testis, where high expression of *Bscl2* mRNA was observed, were significantly reduced in SKO rats.

SKO rat develops generalized lipodystrophy

Dissection and computer tomography of SKO rat revealed the lack of WAT throughout the body (Fig 2A and B). Body composition analysis demonstrated that fat mass in both subcutaneous and intra-abdominal areas was markedly reduced while lean mass was obviously increased in SKO rats (Supplementary Material, Fig. S2A). Enlargement of skeletal muscle was confirmed by magnetic resonance imaging (MRI) (Supplementary Material, Fig. S2B). In fact, the size of epididymal WAT that is one of intra-abdominal adipose tissues and subcutaneous oil red O staining positive area were extremely reduced in SKO rats although small lipid droplets were detected in both regions (Supplementary Material, Fig. S2C and D). Consistent with this, plasma leptin concentration was markedly decreased in SKO rats compared with WT rats (Fig. 2C). BSCL2 patients lack not only the 'metabolically active' adipose tissue such as subcutaneous and intra-abdominal ones but also the 'mechanical' adipose tissue located in the bone marrow and retro-orbital areas (7,21). No adipose tissue was detected in the bone marrow and retro-orbital areas in SKO rats (Supplementary Material, Fig. S2E and F).

In contrast to WAT, interscapular brown adipose tissue (BAT) remained certain (Supplementary Material, Fig. S3A), although its weight was decreased in SKO rats (Fig. 1F). To examine whether the BAT in SKO rats is functional, we conducted cold

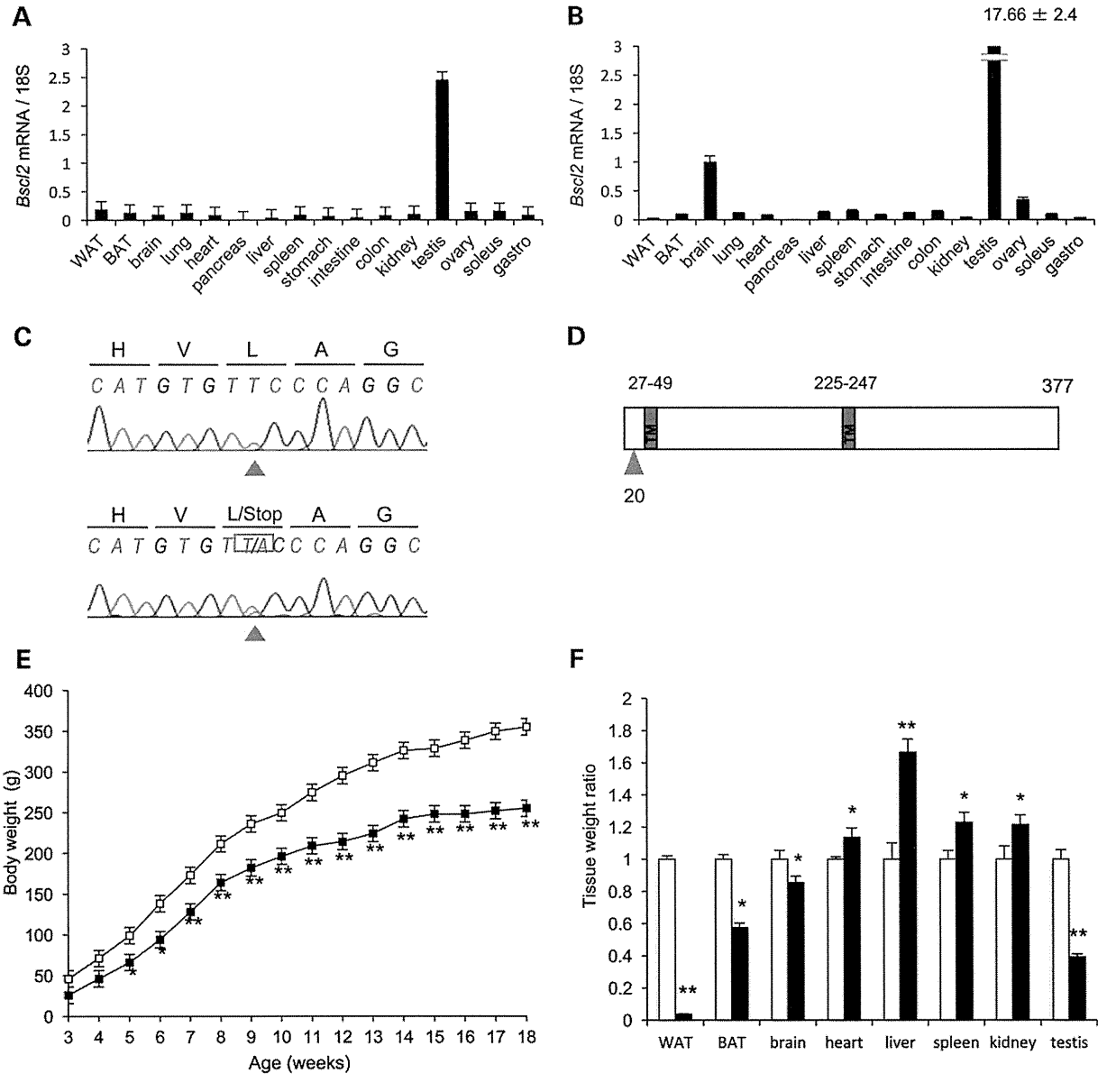

Figure 1. Development of BSCL2 animal model. (A and B) *Bscl2* mRNA expressions in various tissues in 20-week-old male mice (A) and rats (B) were checked with quantitative RT–PCR. *Bscl2* mRNA expression levels were normalized by 18S. Values are means ± SEM ($n = 10$). (C) Normal sequence and heterozygous T to A mutation at nucleotide 239 (red arrows) of *Bscl2* gene in WT and G1 male offspring heterozygous mutant rats, respectively. (D) Schematic diagram of seipin that consists of two transmembrane domains. The red arrow indicates the amino acid position of the L20X mutation. (E) Growth curve of body weight in male SKO rats (filled square) and their WT littermates (open square). Values are means ± SEM ($n = 10$ per group). *$P < 0.05$, **$P < 0.01$ (ANOVA). (F) Weights of various tissues in 20-week-old male SKO rats (closed bars) and their WT littermates (open bars). The fold change is displayed as relative to WT rats. Values are mean ± SEM ($n = 10$ per group). *$P < 0.05$, **$P < 0.01$, NS, not significant (Student's *t*-test).

exposure experiment. Twenty-four hours exposure of 4°C did not change the body temperature in both SKO and WT rats (Supplementary Material, Fig. S3B). At this time, interscapular BAT weight was similarly decreased in SKO and WT rats (Supplementary Material, Fig. S3C). Histological analysis revealed the reduction of lipid droplet number after 24 h cold exposure especially in SKO rats (Supplementary Material, Fig. S3D). In addition, increment of *Ucp1* mRNA expression by cold exposure was not just observed in both SKO and WT rats but was greater in SKO rats than in WT rats (Supplementary Material, Fig. S3E). These results indicate that the BAT in SKO rats was, in terms of thermogenesis, physiologically functional.

IPGTT showed impaired glucose tolerance with hyperinsulinemia, indicating insulin resistance, in SKO rats (Fig. 2D). Under ad lib feeding, plasma triglyceride concentration was markedly elevated in SKO rats while plasma non-esterified fatty acid (NEFA) concentration was unchanged (Fig. 2E and Supplementary Material, Fig. S4A). Plasma total cholesterol (T-Chol) was also elevated in SKO rats (Supplementary Material, Fig. S4B). We studied the effect of fasting on SKO rats. During a 24 h fasting,

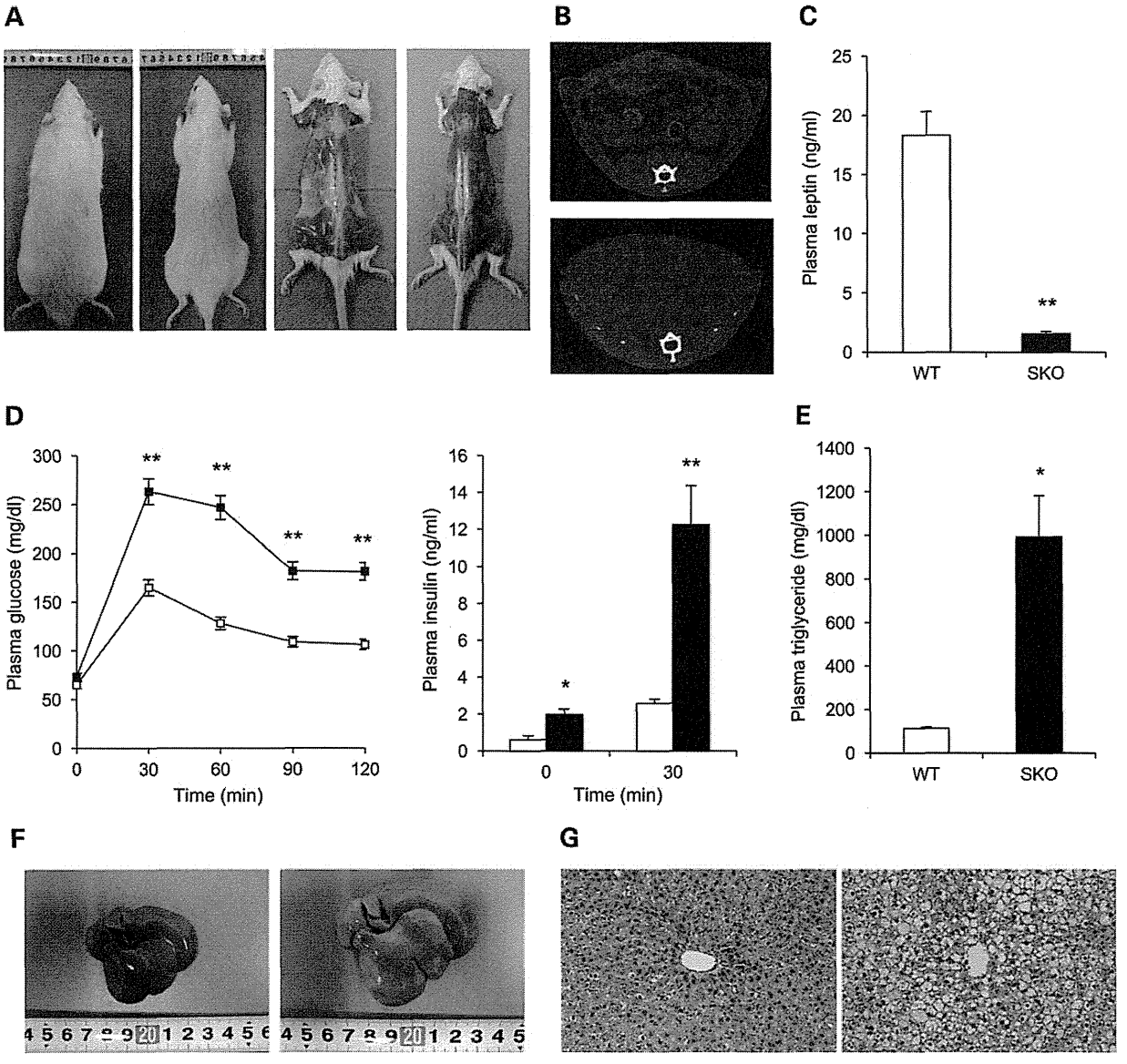

Figure 2. SKO rat develops generalized lipodystrophy. (A) Gross appearance of dorsal view before and after removal of skin in a 20-week-old male SKO rat (right) and its WT littermate (left). (B) Computer tomography image at a slice 15 cm distal from nose in a SKO rat (bottom) and its WT littermate (top). (C) Plasma leptin concentrations in SKO rats (closed bars) and their WT littermates (open bars). (D) Plasma glucose (left panel) and plasma insulin concentrations (right panel) during IPGTT in SKO rats (filled squares or closed bars) and their WT littermates (open square or open bars). (E) Plasma triglyceride concentrations in SKO rats (closed bars) and their WT littermates (open bars). (C–E) Values are means ± SEM ($n = 10$ per group). *$P < 0.05$, **$P < 0.01$, NS, not significant (Student's t-test). (F and G) Macroscopic (F) and histological images (G) of the liver in a SKO rat (right) and its WT littermate (left). For histological examination, hematoxylin and eosin staining was used. Original magnification of ×200 is shown.

both SKO and WT rats lost body weight (Supplementary Material, Fig. S5A). Glucose concentration dropped slightly in WT rats, but plummeted in SKO rats to WT levels (Supplementary Material, Fig. S5B). Insulin concentration also dropped in both SKO and WT rats although its level was still higher in SKO rats than in WT rats (Supplementary Material, Fig. S5C). Under these conditions, NEFA concentration appropriately increased in WT rats as a normal respond to fasting, meanwhile it did not increase but dropped in SKO rats, indicating that SKO rats had no sufficient lipid stores to respond to fasting (Supplementary Material, Fig. S5D). Since circulating NEFA is metabolized to ketone bodies, such as β-hydroxybutyrate, by the liver, we checked β-hydroxybutyrate concentrations. Consistent with the results of NEFA, β-hydroxybutyrate concentration vastly increased in WT rats but did not in SKO rats (Supplementary Material, Fig. S5E).

The liver in SKO rats was remarkably enlarged and was lighter in color, suggesting severe fatty liver (Fig. 2F). Histological examination showed large number of lipid droplets of various sizes in SKO rats (Fig. 2G). Consistent with these results, liver weight and liver TG content were also remarkably increased in SKO rats (Supplementary Material, Fig. S4C and D).

These results demonstrate that SKO rats develop generalized lipodystrophy and its related phenotypes, which are strikingly similar to those of human BSCL2.

SKO rat develops impairment of spatial working memory

We evaluated the spatial working memory by Y-maze test for the assessment of mental development in SKO rats. Y-maze score was significantly lower in SKO rats than that in WT rats (Fig. 3A) while spontaneous movement was unchanged. To determine whether this impairment of spatial working memory is seipin knockout specific, we performed the same experiment in leptin-deficient Lep^{mkyo}/Lep^{mkyo} rats and A-ZIP/F-1 mice, a mouse model of generalized lipodystrophy due to adipocyte specific expression of dominant negative protein for b-zip protein (22). Both Lep^{mkyo}/Lep^{mkyo} rats and A-ZIP/F-1 mice showed no significant change in Y-maze score when compared with their WT littermates, respectively, indicating that the impairment of spatial working memory in SKO rats is due to neither leptin deficiency nor lipodystrophy (Fig. 3B and C).

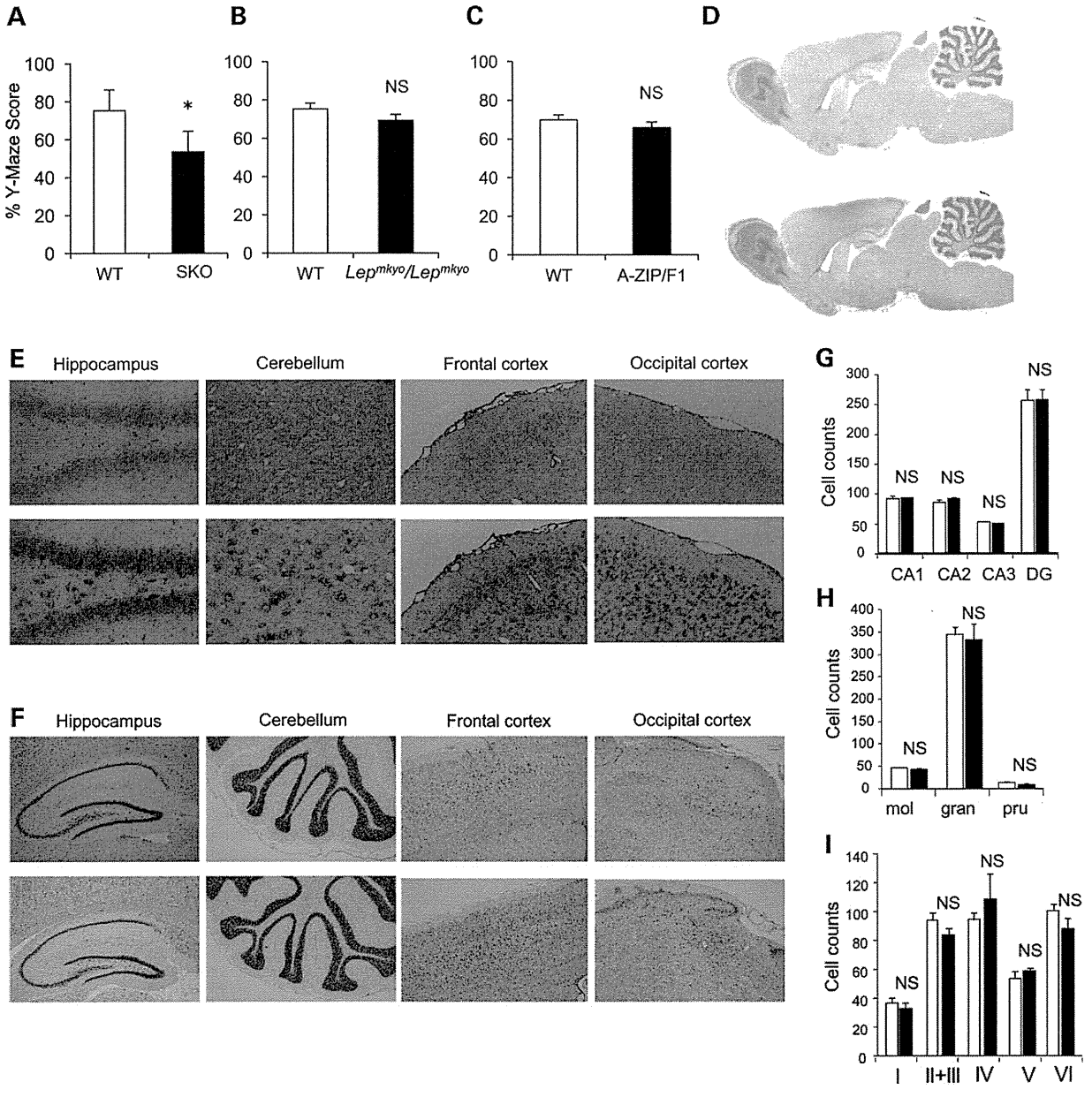

Figure 3. The role of seipin in the brain development. (A–C) Y-maze score as an index of spatial working memory in SKO rats (A), Lep^{mkyo}/Lep^{mkyo} rats (B) and A-ZIP/F-1 mice (C). Values are mean ± SEM ($n = 10$ per group). *$P < 0.05$, NS, not significant (Student's t-test). (D and E) *Bscl2* expression pattern in the whole brain (D) and sections (E) of hippocampus, cerebellum, frontal cortex and occipital cortex assessed by *in situ* hybridization in a WT rat. Images used with sense probe (top) and antisense probe (bottom) are shown. Original magnification of ×16 is shown for the whole brain. ×200 is for hippocampus and cerebellum and ×100 is for frontal and occipital cortexes. (F) Microscopic images of hippocampus, cerebellum, frontal cortex and occipital cortex in WT (top) and SKO rats (bottom). Nissl staining was used. Original magnification of ×40 is shown. (G–I) The number of Nissl stained cells in four regions (CA1, CA2, CA3, DG) of hippocampus (G), five layers (I, II+III, IX, V, VI) of frontal cortex (H) and three layers (molecular cell layer, granular cell layer and Purkinje cell layer) of cerebellum (I) in SKO rats (closed bars) and their WT littermates (open bars). Values are means ± SEM ($n = 9$ per group). NS, not significant (Student's t-test).

The role of seipin in the brain development

Gene expression pattern of *Bscl2* in the whole brain was analyzed by *in situ* hybridization in WT rats. *Bscl2* gene was ubiquitously expressed throughout the brain including hippocampus, cerebellum and, frontal and occipital cortex in WT rats (Fig. 3D and E). Next, we histologically examined of the brain in SKO rats. In comparison with WT rats, any morphological changes were not detected throughout the brain in SKO rats (Fig. 3F). Since the whole brain weight was slightly but significantly decreased in SKO rats (Fig. 1F), we examined the neuron density in hippocampus, cerebellum and frontal cortex. In any layers or regions of these sections, no significant change of neuron density was detected (Fig. 3G–I). The fact that the brain volume was decreased while neuron density was unchanged means that the total neuron number in the brain was decreased.

Intellectual quotient test and brain volume in human BSCL2 patient

Intellectual quotient test was examined in two male and four female BSCL2 patients. The age of these six patients was ranging from 18 to 36 years (Supplementary Material, Table. S1). Four patients had R275X, one patient had E189X and the remaining one had Y187C homozygous mutation in *BSCL2* gene, respectively. Five of six patients showed mild but obvious reduction in both verbal and performance intelligence quotient scores. Brains of the same six patients were examined by MRI. No apparent morphological change was reported with these MRI examinations in any patients. For the analysis of brain volume, three male and six female healthy subjects whose age was ranging from 21 to 34 years (mean, 25.4 years) with normal body mass index between 18.5 and 25.0 kg/m^2 were also examined by MRI. With the small number of subjects, we found no significant difference but the tendency of reduction in whole brain volume in the patients when compared with healthy subjects (Fig. 4A). Next, we checked the brain parenchymal area of coronal sections at three different levels. In two of the three sections, significant reduction of brain parenchymal area was observed in the patients (Fig. 4B). Finally, we checked the brain parenchymal /subarachnoid area ratio to assess the presence of brain atrophy. No significant difference of this ratio was observed at any levels between the patients and healthy subjects, indicating that the reduction of brain volume in BSCL2 patients was not due to brain atrophy (Fig. 4C).

Male SKO rat shows infertility with azoospermia

Although serum levels of hormones including lutenizing hormone (LH), follicle stimulation hormone (FSH) and testosterone, in male SKO rats were all within normal range and showed no significant difference from those in male WT rats (Supplementary Material, Fig. S7), male SKO rats showed remarkably small testis in weight when compared with WT rats (Fig. 5A and D) and were infertile while female SKO rats were fertile. There was no significant change in testis weight in both Lep^{mkyo}/Lep^{mkyo} rats and A-ZIP/F-1 mice when compared with that in their WT littermates, respectively (Fig. 5B–E). Testis histology showed markedly shrunk spermatic duct and lack of mature sperm cells in SKO rats while there was no change in both Lep^{mkyo}/Lep^{mkyo} rats and A-ZIP/F-1 mice when compared with their WT littermates (Fig. 5D and E). These results indicate that azoospermia in SKO rats is due to neither leptin deficiency nor lipodystrophy.

The role of seipin in the spermatogenesis

Gene expression of *Bscl2* in testis was analyzed with two infertile mouse models. One was Sl/Sl^d mutant mouse that has Sertoli cell dysfunction and the other was W/W^v mutant mouse that has lack of functional C-Kit (23,24). *Bscl2* gene expression was detected in WT mice but not in Sl/Sl^d and W/W^v mice, indicating that *Bscl2* gene is expressed in neither Sertoli nor Spermatogonia cells (Fig. 5F). Gene expression of *Bscl2* during the period of postnatal development in WT rat testis was examined and the significant increment was detected from 5 to 6 weeks (Fig. 5G). Most rats reach sexual maturity at 6 or 7 weeks old. Finally, gene expression pattern of *Bscl2* in testis was analyzed by *in situ* hybridization in WT rats (Fig. 5H). *Bscl2* gene was expressed in spermatocytes and mature sperm cells but not in spermatogonia cells. These results indicate that seipin might have an important role especially in the late phase of spermatogenesis.

Semen examination and gonadal hormone concentrations in human BSCL2 patients

Semen and gonadal hormone concentrations were examined in two male patients with BSCL2. On semen examination, one patient showed obvious oligospermia and the other patient showed normal but minimum of the normal range value in all parameters (Table 1). On the other hand, gonadal hormone

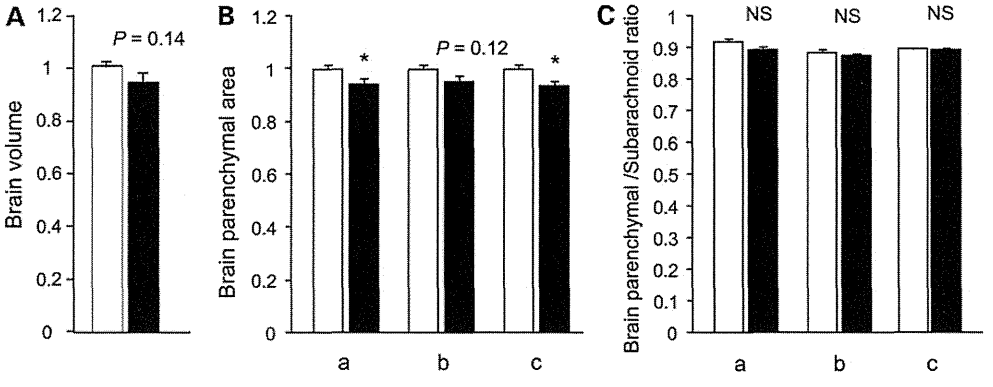

Figure 4. MRI analysis of brain volume in human BSCL2 patients. (A) Whole brain volume in BSCL2 patients (closed bar) and healthy subjects (open bar). The fold change was displayed as relative to healthy subjects. (B) Brain parenchyma area of coronal sections at three different levels in BSCL2 patients (closed bar) and healthy subjects (open bar). (C) Brain parenchyma/subarachnoid area ratio at three different levels in BSCL2 patients (closed bar) and healthy subjects (open bar). Three different levels: (a) the level just above the bilateral ventricles, (b) the level in the center of the lateral ventricles, (c) the level through interventricular foramen. Values are mean ± SEM (Healthy subjects; $n = 9$, BSCL2 patients; $n = 6$). *$P < 0.05$, **$P < 0.01$, NS, not significant (Student's t-test).

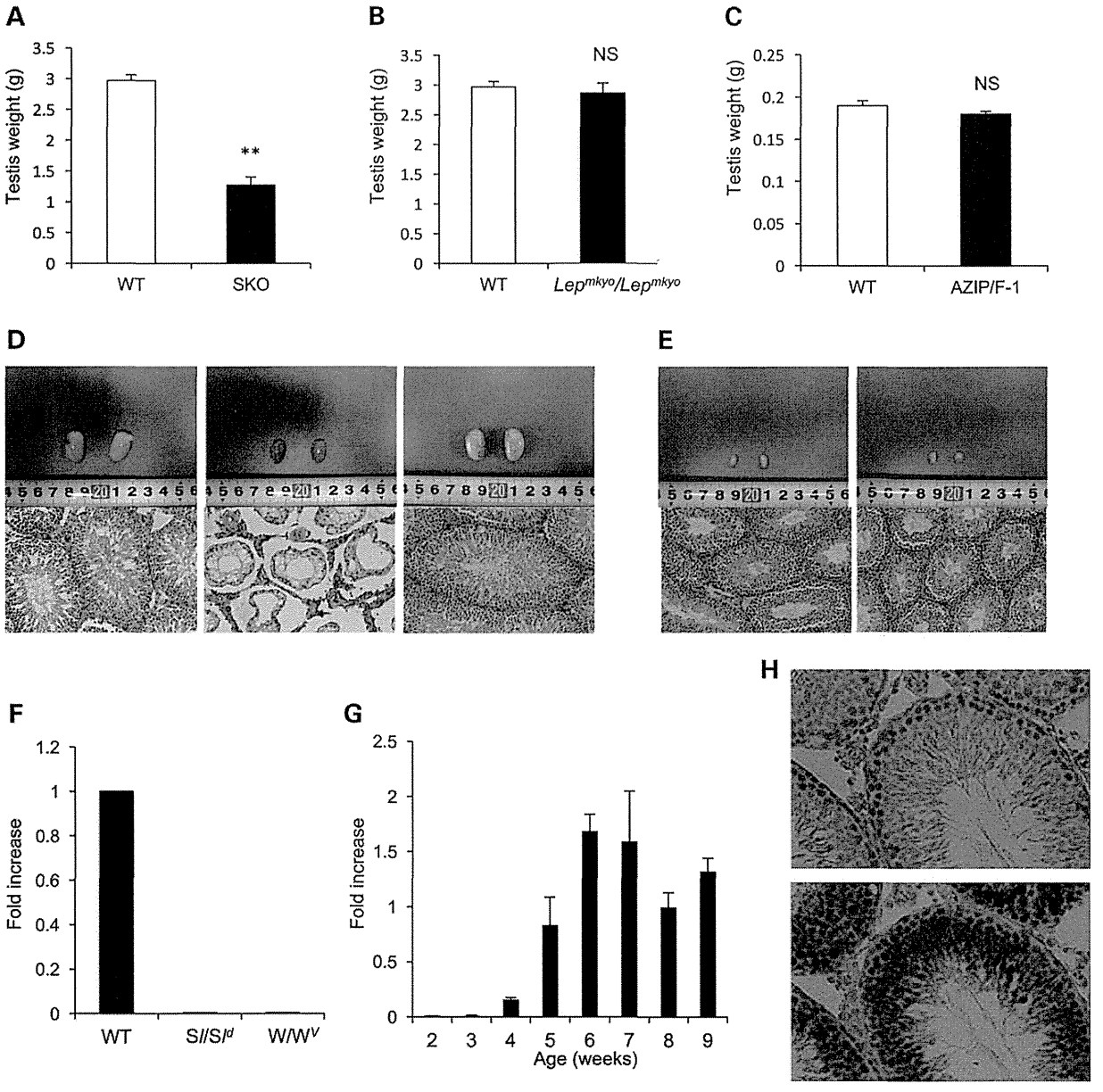

Figure 5. The role of seipin in the spermatogenesis. (A–C) Testis weight in SKO rats (A), *Lep*^{mkyo}/*Lep*^{mkyo} rats (B) and A-ZIP/F-1 mice (C). Values are mean ± SEM ($n = 10$ per group). $^{**}P < 0.01$, NS, not significant (Student's *t*-test). (D and E) Macroscopic (top) and histological images (bottom) of the testis in WT (left), SKO (middle) and *Lep*^{mkyo}/*Lep*^{mkyo} (right) rats (D), and WT (left) and A-ZIP/F-1 (right) mice (E). For histological examination, hematoxylin and eosin staining was used. Original magnification of ×40 is shown. (F) *Bscl2* mRNA expressions checked with quantitative RT–PCR in the testis in 12-week-old WT, Sl/Sl^{d} and W/W^{v} mice. The fold change is displayed as relative to WT mice. $n = 6$ per group. (G) *Bscl2* mRNA expressions checked with quantitative RT–PCR in the testis during the period of postnatal development in WT rats. Values are mean ± SEM ($n = 6$ per group). (H) *Bscl2* expression pattern in the testis assessed by *in situ* hybridization in a WT rat. Images used with sense probe (top) and antisense probe (bottom) are shown. Original magnification of ×200 is shown.

concentrations including LH, FSH, testosterone and prolactin were within normal range in both patients (Supplementary Material, Table. S2). Although further study is needed, these results suggest the potential involvement of seipin in spermatogenesis in human.

Discussion

Using gene-driven ENU mutagenesis, we generated seipin deficient SKO rat. The mutation of *Bscl2* gene in SKO rats (*Bscl2*^{sko}) is located at nucleotide 239 in the third exon of *Bscl2*, generating a stop codon at amino acid 20 (L20X). Seipin has two distinct hydrophobic amino acid stretches and is speculated to have two transmembrane domains (1). L20X mutation is located upstream of these two transmembrane domains. In patients with lipodystrophy, nearly 30 *BSCL2* mutations have been reported so far (25). Among these *BSCL2* mutations, R275X mutation is the closest to the C-terminal (7). No relationship between the location of mutation site and severity of lipodystrophy is found, indicating that the region from the position at amino acid 275 to the C-terminal

Table 1. Semen examination in human BSCL2 patients

Variables	Patient 1	Patient 2	Cut-off value in WHO manual (2010)
Age	21	25	
Volume (ml)	3.6	1.5	1.5
Concentration (10^6/ml)	20	10	15
Total sperm number (10^6/ejaculate)	72	15	39
Motility (% motile)	75	60	40

is important for the physiological function of seipin. SKO rat that has a nonsense mutation located upstream of the two transmembrane domains is considered to have no functional seipin.

The mean mutation frequency with ENU mutagenesis of our protocol was one mutation per 3.7 million base pairs (20). Although the chance for the occurrence of an unexpected mutation with a phenotypic effect is relatively small, this possibility also should be taken account for the experimental design and interpretation of the results. To eliminate mutations that might have been generated by ENU in chromosomal regions other than the *Bscl2* locus, we performed backcross more than six generations against F344/NSlc inbred background, and we always compared phenotypes between littermates to minimize the effect of possible unexpected mutation.

The body weight in SKO rats was significantly lower than that in their WT littermates (Fig. 2A). Body composition analysis with computer tomography revealed that fat mass in both subcutaneous and intra-abdominal areas was markedly reduced while lean mass was obviously increased in SKO rats (Supplementary Material, Fig. S2A). In human patients with BSCL, organomegaly such as hepatosplenomegaly, cardiomegaly and muscular hypertrophy is generally observed as a consequence of hyperinsulinemia (17). We therefore compared weights in various tissues between SKO and WT rats and found that weights of the brain and the testis were significantly decreased in SKO rats in addition to the white and brown adipose tissues although weights of many other tissues were increased in SKO rats (Fig. 1F). Taking together with the fact that *Bscl2* mRNA is highly expressed in the brain and the testis (Fig. 1B), it was strongly suggested that seipin has an important role in the development of these two organs.

Patients with BSCL2 mutation have the most severe variety of BSCL (13,25,26). They lack not only the 'metabolically active' adipose tissue such as subcutaneous and intra-abdominal ones but also the 'mechanical' adipose tissue located in the retro-orbital, bone marrow and so on (7,21). SKO rats lost more than 95% of fat mass in both subcutaneous and intra-abdominal areas (Supplementary Material, Fig. S2A), while more than 20% of fat mass in WT control mice was preserved in seipin knockout mice (14,15). We also confirmed no detectable adipose tissue in the bone marrow and retro-orbital areas in SKO rats by histological examination (Supplementary Material, Fig. S2E and F). On the other hand, even in BSCL2 patients, examination of subcutaneous biopsies found small adipocytes with low but detectable lipid content (27). In SKO rats, small adipocytes with small oil red O stained lipid droplets were also observed (Supplementary Material, Fig. S2D). SKO rat is a perfect model of human BSCL2 in terms of lipodystrophy and might be a useful model for the analysis of physiological roles of seipin in adipogenesis. We have already started the investigation with primary cultures of fibroblasts from SKO rats.

Lipodystrophy-associated phenotypes of SKO rats are also strikingly similar to those of human BSCL2 patients. Patients with severe lipodystrophy like BSCL2 generally exhibit insulin resistant but non-ketotic diabetes, hypertriglyceridemia, fatty liver, organomegaly and increased metabolic rate (17,26). While SKO rats had hyperglycemia with hyperinsulinemia (Fig. 3D), they did not have increased b-hydroxybutyrate level at baseline and fasting failed to increase it (Supplementary Material, Fig. S5E). Unlike *Bscl2* knockout mice (14–16), triglyceride level was markedly elevated in SKO rats (Fig. 3E). While it was reported that the expression of LDL-receptor in the liver was increased in *Bscl2* knockout mice (16), LDL-receptor mRNA expression was unchanged in SKO rats (data not shown). This might be the reason for the difference of triglyceride metabolism between mice and rats. Most organs except for adipose tissues, brain and testis were enlarged in SKO rats (Fig. 2B). Moreover, energy expenditure was increased in SKO rats as the oxygen consumption indicated (Supplementary Material, Fig. S1C). In contrast, *Bscl2* knockout mice showed a decrease in energy expenditure (16). The generation of SKO rat provided us a powerful tool for studying the pathophysiology of human BSCL2.

BSCL2 patients exhibit much higher rates of mild mental retardation than do patients with other BSCL genotypes (13). Although these cognitive defects were speculated to relate to the high expression of Bscl2 mRNA in the brain, it was also possible that the lack of adipose tissue contributes to the mental retardation. Furthermore, it had been reported that leptin secreted from adipocytes plays a role in the regulation of cognitive function (28,29). BSCL2 patients present with the most severe lipodystrophy and their leptin levels are extremely low. In this study, we evaluated the spatial working memory by Y-maze test not only in SKO rats but also leptin deficient Lep^{mkyo}/Lep^{mkyo} rats and A-ZIP/F-1 mice, a mouse model of generalized lipodystrophy and clearly revealed that the impairment of spatial working memory observed in SKO rats is due to neither leptin deficiency nor lipodystrophy (Fig. 3A–C). The spatial working memory of the rodents is responsible for recording information about the environment and the spatial orientation (30). In behavioral science, Y-maze is used to investigate how rodents function with spatial working memory from the early 20th century (31). This is the first report demonstrating that seipin deficiency itself leads to cognitive defect *in vivo*.

To identify the original region responsible for the impairment of spatial working memory in SKO rats, we examined the distribution of *Bscl2* mRNA expression in the whole brain by *in situ* hybridization in WT rats. *Bscl2* mRNA was ubiquitously expressed throughout the rostral–caudal extent of the rat brain including hippocampus, cerebellum, frontal and occipital cortex (Fig. 3D and E). Then, we compared the brain histologically between WT and SKO rats but we could not find any morphological changes throughout the brain (Fig. 3F). Next, we examined the neuron density in hippocampus, cerebellum and frontal cortex, there was no significant difference between WT and SKO rats in any layers or regions of these areas (Fig. 3G–I). These results and the fact that the whole brain volume was significantly reduced in SKO rats indicate that the total neuron number of the brain was decreased in SKO rats. No evidence of brain atrophy suggests that the cause of the reduction of neuron number is a suppression of neuron increment rather than a stimulation of neuron decrease such as apoptosis. Furthermore, no evidence of morphological abnormality suggests that the suppression of neuron increment might be due to disorder of neuron proliferation rather than disorder of neuron differentiation. The causal relationship between brain volume reduction and impairment of cognitive function in SKO rats is unclear since the present study did not deny the possibility

that seipin has a role in the neuronal function. In this study, we also found the reduction of brain volume in human BSCL2 patients although we need further study with more large number of patients to confirm it (Fig. 4A–C). Ventricular dilatation in CGL patients whose etiology was unknown was reported by pneumoencephalography (17). However, the ratio of subarachnoid area including cerebral ventricles to parenchymal area assessed by MRI in our patients showed no significant difference with that in healthy controls (Fig. 4C), demonstrating that our patients had no ventricular dilatation. In addition, while malformation of the hypothalamus in a CGL patient was also reported (32), all MRI images were assessed by radiologists and no morphological abnormality was pointed out in the present study. This is the first report indicating the pathophysiological role of seipin in the brain development in both rats and humans. Any apparent phenotypes of motor neuron disease that is associated with gain-of-toxic-function mutation in the N-glycosylation site of seipin (33) were not observed in both SKO rats and our BSCL2 patients.

SKO rats showed infertility with azoospermia. Testis weight was remarkably reduced and testis histology showed markedly shrunk spermatic duct and lack of mature sperm cells in SKO rats (Fig. 5D). These testis phenotypes were not observed in *Lep*$^{mkyo/Lepmkyo}$ rats and A-ZIP/F-1 mice, clearly indicating that the azoospermia observed in SKO rats is due to neither leptin deficiency nor lipodystrophy. Serum concentrations of gonadal hormones including LH, FSH and testosterone in SKO rats were all within normal range and were not significantly different from those in WT rats (Supplementary Material, Fig. S7). *Bscl2* mRNA is highly expressed in the testis. These facts indicate that the responsive region for the azoospermia in SKO rats is the testis itself. Analyses using with Sl/Sl^{d} and W/W^{v} mice demonstrated that *Bscl2* mRNA is expressed in neither Sertoli nor Spermatogonia cells. In addition, the analysis during the period of postnatal development in WT rats demonstrated that the significant increment of *Bscl2* mRNA expression was detected only from 5 to 6 weeks. WT rat produces mature sperm cells from the age of 6 or 7 weeks old. Consistent with these results, analysis of WT rat testis by *in situ* hybridization showed that *Bscl2* mRNA was not expressed in spermatogonia cells. These results indicate that seipin has an important role in the late phase of spermatogenesis in rats.

At least one male BSCL2 patient has been reported with multiple healthy children (17,25). However, semen examination in this patient was not reported. Recently, one other male BSCL2 patient was reported to have teratozoospermia (19). There was also no information on the number of sperm in this patient. In this study, we performed semen examination in two BSCL2 male patients and found that one patient had oligospermia according to the WHO criteria and the other had low sperm concentration but above the cut-off value of the criteria. Although further study is required, these results suggest the potential involvement of seipin in spermatogenesis in human.

In conclusion, through the generation and analysis of SKO rat, a rat model of BSCL2, we found that seipin deficiency leads to impairment of cognitive function with brain weight reduction and infertility with azoospermia in addition to generalized lipodystrophy, those have not been reported in seipin KO mice. We also confirmed reduction of brain volume and number of sperm in human patients with *BSCL2* mutation although further study is needed to clarify human phenotypes. This is the first report demonstrating that seipin is necessary for normal brain development and spermatogenesis in addition to white adipose tissue development.

Materials and Methods

Animals

Rats with a *Bscl2* mutation were obtained by ENU mutagenesis of F344/NSlc rats, followed by MuT-POWER (Mu Transposition POoling method With sequencER) screening on the genomic DNA of 4608 G1 male offspring in KURMA (Kyoto University Rat Mutant Archive). ENU mutagenesis procedures, screening protocols (20) and intracytoplasmic sperm injection procedure were previously described (34) The forward primer and the reverse primer used for identifying mutation of *Bscl2* were 5′-GATGTTGCTTTGT CCTGCTA-3′ and 5′-TTTCTCGGTTTTTCACCAC-3′, respectively. More than six backcross generations were performed against the F344/NSlc inbred background. Genotyping for *Bscl2*^{sko}mutation was performed by real-time PCR system using TaqMan Sample-to-SNP kit (Applied Biosystems, Carlsbad, CA, USA) with a specific primer pair (Forward primer sequences are 5′-TGTGGG CCCAGGAAGTG-3′ and reverse primer sequences are 5′-CCCCA AACTGCAGCATCAG-3′) and TaqMan MGB probes (WT probe sequences are 5′-CCTGCCTACACATGG-3′ and mutant probe sequences are 5′-CCTGCCAACACATGG-3′). Genomic DNA was extracted from whole blood. The cycling conditions were 20 s at 95°C followed by 40 cycles of 3 s at 95°C and 20 s at 60°C. F344/NSlc rats and C57Bl/6J mice were purchased (Japan SLC, Hamamatsu, Japan). *Lep*^{mkyo}/ *Lep*^{mkyo} rats on F344/NSlc background were generated previously (35). A-ZIP/F-1 mice were provided from Diabetes Branch, National Institute of Diabetes and Digestive and Kidney Diseases (Bethesda, MD, USA) (22). Sl/Sl^{d} mice and W/W^{v} mice were purchased from Japan SLC. Rats and mice were maintained on a 14 h light/10 h dark cycle (lights on 7:00 AM, lights off 9:00 PM) and fed ad libitum standard pellet diet (MF; Oriental Yeast, Tokyo, Japan).

All animal care and experiments conformed to the Guidelines for Animal Experiments at Kyoto University and were approved by the Animal Research Committee of Kyoto University.

Real-time quantitative RT–PCR for Bscl2 mRNA expression

Each tissue was frozen in liquid nitrogen and stored at −80°C until use for RNA isolation. RNA was prepared using Trizol (Invitrogen, Carlsbad, CA, USA) reagent following the supplier's protocol. The Quality and the concentrations of the extracted RNA were checked using the Nano-Drop 2000 (Thermo Scientific, Yokohama, Japan). Single-stranded cDNA was synthesized from 1 μg of total RNA using SuperScript III First-Strand Synthesis System for RT–PCR, according to the manufacturer's instructions (Invitrogen). Quantitative RT–PCR was performed with SYBR Green (Applied Biosystems) by Applied Biosystems StepOnePlus™ RT–PCR System using gene specific primer. The housekeeping rat or mouse mitochondrial subunit 18S rRNA genes were used for control and quantitative RT–PCR was performed with TaqMan (Applied Biosystems). The sequences of primers (Sigma-Genosys, Tokyo, Japan) used in the present study are as follows: rat *Bscl2* forward; 5′-CCCACAAGTGATTTGAGTTGGGGA-3′, rat *Bscl2* reverse; 5′-GTGGCTGACGGTCGGCATGT-3′, mouse *Bscl2* forward; 5′-GGTTCT CGCCGCTTACGTTGCG-3′, mouse *Bscl2* reverse; 5′-GGTCTCCCAGC TCGCGTCACT-3′, rat 18s forward; 5′-GCAATTATTCCCCATGAAC GA-3′, rat 18s reverse; 5′-CAAAGGGCAGGGACTTAATCAAC-3′, probe; 5′-AATTCCCAGTAAGTGCGGGTCATAAGCTTG-3′, mouse 18s forward; 5′-CGCGCAAATTACCCACTCCCGA-3′, mouse 18s reverse; 5′-CGGCTACCACATCCAAGGA-3′, probe; 5′-CCAATTA CAGGGCCTCGAAA-3′.

Computed tomography

Computed tomography (CT) image of 20-week-old male rats was obtained under anesthesia by La Theta LCT-100 (Aloka, Tokyo, Japan).

Biochemical assays

Blood was obtained from the tail vein under ad libitum feeding at the age of 20 weeks if not otherwise specified. Plasma leptin concentrations were measured by an enzyme-linked immunosorbent assay (ELISA) kit for rat leptin (Millipore, St Charles, MO, USA). Plasma glucose concentrations were measured by a glucose assay kit (Wako Pure Chemical Industries, Osaka, Japan). Plasma insulin concentrations were measured by an insulin-ELISA kit (Morinaga Institute of Biological Science, Yokohama, Japan). Plasma triglyceride concentrations were measured by an enzymatic kit (Triglyceride E-test Wako; Wako Pure Chemical Industries).

Glucose tolerance test

Intraperitoneal glucose tolerance test (IPGTT) was performed after overnight fasting in 20-week-old male rats. Rats received 2.0 mg/g glucose by intraperitoneal injection. Blood was sampled from the tail vein before and 15, 30, 60, 90, 120 min after the glucose load.

Histology

Rat livers and rat and mouse testes were fixed in 10% neutrally buffered formalin and subsequently embedded in paraffin. Histological sections of 5 mm thickness were stained with hematoxylin and eosin. Rat brains were sampled after perfusion with 4% paraformaldehyde under anesthesia by intraperitoneal injection of sodium pentobarbital (DS Pharma Biomedical, Suita, Japan), fixed in 4% paraformaldehyde and subsequently embedded in paraffin. Sagital sections of 4 mm thickness were Nissl stained with 0.1% Cresyl violet solution.

Y-maze test

Spatial working memory was assessed by the Y-maze test in 20-week-old male SKO rats, Lep^{mkyo}/Lep^{mkyo} rats and A-ZIP/F-1 mice as described previously (36). Briefly, the Y-maze test was conducted during the dark period (9:00 PM to 11:00 PM) in a dimly illuminated room. The maze consists of three arms (for rats; 425 mm long, 225 mm high and 145 mm wide, for mice; 300 mm long, 150 mm high and 60 mm wide, labeled A, B or C) diverging at a 120° from the central point. Each rat was placed at the end of the start arm and allowed to move freely through the maze during an 8-min session. The sequence of arm entries was manually recorded. An actual alternation was defined as entries into all the three arms on consecutive occasions. The maximum alternation was subsequently calculated by measuring the total number of arm entries minus 2 and the percentage of alternation was calculated as (actual alternations/maximum alternations) ×100. The total number of arms entered during the sessions, which reflect locomotor activities, was also recorded.

In situ hybridization of Bscl2 mRNA

In situ hybridization was performed as described previously (37). Briefly, to prepare cRNA probes, cDNA fragments encoding rat *Bscl2* (NM_001012171.1 sequence166–1092) was amplified. Digoxigenin-labeled sense and antisense probes were synthesized with RNA polymerases. To obtain paraffin-embedded blocks and sections of rat brain and testis, rats were dissected after its perfusion. Rat brains and testes were fixed in 4% paraformaldehyde and embedded in paraffin. Sections of 6 mm thickness were deparaffinized, fixed, hydrogen chloride treated. Hybridization was performed with antisense or sense probe (100 ng/ml) at 60°C for 16 h in hybridization solution (Genostaff, Tokyo, Japan). Hybrids were detected with anti-DIG alkaline phosphate-conjugated antibody (Roche Diagnostics GmbH, Basal, Switzerland) and coloring reactions were performed with NBT/BCIP solution (Sigma-Aldrich Japan, Tokyo, Japan). The sections were counterstained with Kernechtrot stain solution (Muto Pure Chemicals, Tokyo, Japan).

Analysis of cell number in the brain sections

Four regions (CA1, CA2, CA3, DG) of hippocampus and five layers (I, II+III, IX, V, VI) of frontal cortex were photographed at high magnification (×400), respectively (Supplementary Material, Fig. S6A and C). The number of Nissl stained cells in a photographed visual field (0.275 × 0.4125 mm) was counted. The molecular cell layer and granular cell layer of cerebellum were also photographed at high magnification (×400), but the number of stained cells was counted in a smaller visual field (0.13 × 0.4125 mm) (Supplementary Material, Fig. S6B). Purkinje cell layer of cerebellum is a monolayer and the number of stained cells in this layer was just counted in a photograph at high magnification (×400) (Supplementary Material, Fig. S6B).

Measurement of brain size in BSCL2 patients

Brain size of BSCL2 patients was assessed by MRI technique. Whole brain images were acquired by a 3-Tesla Trio MRI scanner (Siemens, Erlangen, Germany) in axial orientation using the following parameters: repetition time, 3000 ms; echo time, 30 ms; flip angle, 90°; voxel size, 3 × 3 × 3 mm; field of view, 192 × 192 mm; matrix size, 64 × 64; and number of slices, 48 (38). Whole brain volume was calculated with the Virtual Place software (AZE, Tokyo, Japan). Brain parenchymal and subarachnoid areas of three different coronal sections, those are just above the bilateral ventricles, in center of the lateral ventricles and through interventricular foramen, were calculated by Image J software (NIH, Bethesda, MD, USA). Study protocols were approved by the Ethical Committee of Kyoto University Graduate School of Medicine. After detailed explanation of the study design, written informed consent was obtained from all subjects before study initiation.

Semen examination in BSCL2 patients

Semen examination was performed in two young adult male BSCL2 patients. One was 24 years old with E189X homozygous mutation and the other was 28 years old with R275X homozygous mutation in *BSCL2* gene. Semen samples were collected by masturbation that followed 3 days of sexual abstinence. Ejaculate volume and concentration of spermatozoa and percentage of motile spermatozoa in semen were analyzed at room temperature immediately after complete liquefaction (2 h). Motility was determined by Cellsoft Automated Semen Analyzer (Cryo Resources, New York, NY, USA).

Statistical analysis

Data are expressed as means ± SEM. Comparison between or among groups was assessed by Student's *t* test or ANOVA with

Fisher's protected least significant difference test. χ^2 test was used for analysis of Mendelian ratios of genotype and sex. $P < 0.05$ was considered statistically significant.

Supplementary Material

Supplementary Material is available at *HMG* online.

Acknowledgements

We thank Takashi Shinohara for discussion and Keiko Hayashi for technical assistance. The authors also acknowledge Yoko Koyama for secretarial assistance.

Conflict of Interest statement. None declared.

Funding

This work was supported by research grants from the Japanese Ministry of Education, Culture, Sports, Science and Technology, the Japanese Ministry of Health, Labor and Welfare, Uehara Memorial Foundation, The European Community's Seventh Framework Programme (FP7/2007–2013) under grant agreement no. HEALTH-F4-2010-241504 (EURATRANS) and Industrial Technology Research Grant Program from New Energy and the Industrial Technology Development Organization (NEDO) of Japan.

References

1. Magré, J., Delépine, M., Khallouf, E., Gedde-Dahl, T. Jr, Van Maldergem, L., Sobel, E., Papp, J., Meier, M., Mégarbané, A., Bachy, A. *et al.* (2001) Identification of the gene altered in Berardinelli-Seip congenital lipodystrophy on chromosome 11q13. *Nat. Genet.*, **28**, 365–370.
2. Capeau, J., Magré, M., Caron-Debarle, M., Lagathu, C., Antoine, B., Bérériat, V., Lascols, O. and Bastard, J.P. (2010) Human lipodystrophies: genetic and acquired diseases of adipose tissue. *Endocr. Dev.*, **19**, 1–20.
3. Garg, A. (2011) Lipodystrophies: genetic and acquired body fat disorders. *J. Clin. Endocrinol. Metab.*, **96**, 3313–3325.
4. Agarwal, A.K., Arioglu, E., De Almeida, S., Akkoc, N., Taylor, S. L., Bowcock, A.M. and Garg, A. (2002) AGPAT2 is mutated in congenital generalized lipodystrophy linked chromosome 9q34. *Nat. Genet.*, **31**, 21–23.
5. Kim, C.A., Delépine, M., Boutet, E., El Mourabit, H., Le Lay, S., Meier, M., Nemani, M., Bridel, E., Leite, C.C., Bertola, D.R. *et al.* (2008) Association of a homozygous nonsense caveolin-1 mutation with Berardinelli-Seip congenital lipodystrophy. *J. Clin. Endocrinol. Metab.*, **93**, 1129–1134.
6. Hayashi, Y.K., Matsuda, C., Ogawa, M., Goto, K., Tominaga, K., Mitsuhashi, S., Park, Y.E., Nonaka, I., Hino-Fukuyo, N., Haginoya, K. *et al.* (2009) Human PTRF mutations cause secondary deficiency of caveolins resulting in muscular dystrophy with generalized lipodystrophy. *J. Clin. Invest.*, **119**, 2623–2633.
7. Ebihara, K., Kusakabe, T., Masuzaki, H., Kobayashi, N., Tanaka, T., Chusho, H., Miyanaga, F., Miyazawa, T., Hayashi, T., Hosoda, K. *et al.* (2004) Gene and phenotype analysis of congenital generalized lipodystrophy in Japanese: a novel homozygous nonsense mutation in seipin gene. *J. Clin. Endocrinol. Metab.*, **89**, 2360–2364.
8. Agarwal, A.K. and Garg, A. (2003) Congenital generalized lipodystrophy: significance of triglyceride biosynthetic pathways. *Trends. Endocrinol. Metab.*, **14**, 214–221.
9. Garg, A. and Agarwal, A.K. (2008) Caveolin-1: a new locus for human lipodystrophy. *J. Clin. Endocrinol. Metab.*, **93**, 1183–1185.
10. Windpassinger, C., Auer-Grumbach, M., Irobi, J., Patel, H., Petek, E., Hörl, G., Malli, R., Reed, J.A., Dierick, I., Verpoorten, N. *et al.* (2004) Heterozygous missense mutations in BSCL2 are associated with distal hereditary motor neuropathy and Silver syndrome. *Nat. Genet.*, **36**, 271–276.
11. Chen, W., Yechoor, V.K., Chang, B.H., Li, M.V., March, K.L. and Chan, L. (2009) The human lipodystrophy gene product Berardinelli-Seip congenital lipodystrophy 2/seipin plays a key role in adipocyte differentiation. *Endocrinology*, **150**, 4552–4561.
12. Ito, D. and Suzuki, N. (2007) Molecular pathogenesis of seipin/BSCL2-related motor neuron diseases. *Ann. Neurol.*, **61**, 237–250.
13. Maldergem, V.L., Magré, J., Khallouf, T.E., Gedde-Dahl, T. Jr, Delépine, M., Trygstad, O., Seemanova, E., Stephenson, T., Albott, C.S. and Bonnici, F. (2002) Genotype-phenotype relationships in Berardinelli-Seip congenital lipodystrophy. *J. Med. Genet.*, **39**, 722–733.
14. Cui, X., Wang, Y., Tang, Y., Liu, Y., Zhao, L., Deng, J., Xu, G., Peng, X., Ju, S., Liu, G. and Yang, H. (2011) Seipin ablation in mice results in severe generalized lipodystrophy. *Hum. Mol. Genet.*, **20**, 3022–3030.
15. Chen, W., Chang, B., Saha, P., Hartig, S.M., Li, L., Reddy, V.T., Yang, Y., Yechoor, V., Mancini, M.A. and Chan, L. (2012) Berardinelli–Seip congenital lipodystrophy 2/seipin is a cell-autonomous regulator of lipolysis essential for adipocyte differentiation. *Mol. Cell Biol.*, **32**, 1099–1111.
16. Prieur, X., Dollet, L., Takahashi, M., Nemani, M., Pillot, B., Le May, C., Mounier, C., Takigawa-Imamura, H., Zelenika, D., Matsuda, F. *et al.* (2013) Thiazolidinediones partially reverse the metabolic disturbances observed in Bscl2/seipin-deficient mice. *Diabetologia*, **56**, 1813–1825.
17. Seip, M. and Trygstad, O. (1996) Generalized lipodystrophy, congenital and acquired (lipoatrophy). Acta Paediatr. Suppl., **413**, 2–28.
18. Zhou, L., Yin, J., Wang, C., Liao, J., Liu, G. and Chen, L. (2014) Lack of seipin in neurons results in anxiety- and depression-like behaviors via down regulation of PPARγ. *Hum. Mol. Genet.*, **15**, 4094–4102.
19. Jiang, M., Mingming, G., Chaoming, W., Hui, H., Kuejiang, G., Zuomin, Z., Hongyuan, Y., Kinhua, X., George, L. and Jiahao, S. (2014) Lack of testicular seipin causes teratozoospermia in men. *Proc. Natl Acad. Sci. USA*, **111**, 7054–7059.
20. Mashimo, T., Yanagihara, K., Tokuda, S., Voigt, B., Takizawa, A., Nakajima, R., Kato, M., Hirabayashi, M., Kuramoto, T. and Serikawa, T. (2008) An ENU-induced mutant archive for gene targeting in rats. *Nat. Genet.*, **40**, 514–515.
21. Simha, V. and Garg, A. (2003) Phenotypic heterogeneity in body fat distribution in patients with congenital generalized lipodystrophy caused by mutations in the AGPAT2 or seipin genes. *J. Clin. Endocrinol. Metab.*, **88**, 5433–5437.
22. Moitra, J., Mason, M.M., Olive, M., Krylov, D., Gavrilova, O., Marcus-Samuels, B., Feigenbaum, L., Lee, E., Aoyama, T., Eckhaus, M. *et al.* (1998) Life without white fat: a transgenic mouse. *Genes. Dev.*, **12**, 3168–3181.
23. Tadokoro, Y., Tomogida, K., Ohta, H., Tohda, A. and Nishiume, Y. (2002) Homeostatic regulation of germinal stem cell proliferation by the GDNF/FSH pathway. *Mech. Dev.*, **113**, 29–39.
24. Ohta, H., Yomogida, K., Dohmae, K. and Nishuume, Y. (2000) Regulation of proliferation and differntiation in spermatogonial cells: the role of c-kit and its ligand SCF. *Development*, **127**, 2125–2131.

25. Cartwright, B.R. and Goodman, J.M. (2012) Seipin: from human disease to molecular mechanism. *J. Lipid. Res.*, **53**, 1042–1055.
26. Garg, A. (2004) Acquired and inherited lipodystrophies. *N. Engl. J. Med.*, **350**, 1220–1234.
27. Rogunum, T.O., Bjerve, K.S., Seip, M., Trygstad, O. and Oseid, S. (1978) Fat cell size and lipid content of subcutaneous tissue in congenital generalized lipodystrophy. *Acta Endocrinol.*, **88**, 182–189.
28. Harvey, J. (2007) Leptin regulation of neuronal excitability and cognitive function. *Curr. Opin. Pharmacol.*, **7**, 643–647.
29. Morrison, C.D. (2009) Leptin signaling in brain: a link between nutrition and cognition? *Biochim. Biophys. Acta*, **1792**, 401–408.
30. O'Keefe, J. and Dostrovsky, J. (1971) The hippocampus as a spatial map. Preliminary evidence from unit activity in the freely-moving rat. *Brain Res.*, **34**, 171–175.
31. Olton, D.S. (1976) Mazes, maps, and memory. *Am. Psychol.*, **34**, 583–596.
32. Berge, T., Brun, A., Hansing, B. and Kjellman, B. (1976) Congenital generalized lipodystrophy. *Acta Pathol. Microbiol. Scand. A.*, **86**, 47–54.
33. Ito, D. and Suzuki, N. (2009) Seipinopathy: a novel endoplasmic reticulum stress-associated disease. *Brain*, **132**, 8–15.
34. Hirabayashi, M., Kato, M., Aoto, T., Ueda, M. and Hochi, S. (2002) Rescue of infertile transgenic rat lines by intracytoplasmic injection of cryopreserved round spermatids. *Mol. Reprod. Dev.*, **62**, 295–299.
35. Aizawa-Abe, M., Ebihara, K., Ebihara, C., Mashimo, T., Takizawa, A., Tomita, T., Kusakabe, T., Yamamoto, Y., Aotani, D., Yamamoto-Kataoka, S. *et al.* (2013) Generation of leptin-deficient Lepmkyo/Lepmkyo rats and identification of leptin-responsive genes in the liver. *Physiol. Genomics.*, **45**, 786–793.
36. Kitamura, A., Fujita, Y., Oishi, N., Kalaria, R.N., Washida, K., Maki, T., Okamoto, Y., Hase, Y., Yamada, M., Takahashi, J. *et al.* (2012) Selective white matter abnormalities in a novel rat model of vascular dementia. *Neurobiol. Aging*, **33**, 25–35.
37. Koizumi, A., Shigemoto-Mogami, Y., Nasu-Tada, K., Shinozaki, Y., Ohsawa, K., Tsuda, M., Joshi, B.V., Jacobson, K.A., Kohsaka, S. and Inoue, K. (2007) Floral development of an asexual and female-like mutant carrying two deletions in gynoecium-suppressing and stamen-promoting functional regions on the Y chromosome of the dioecious plant Silene latifolia. *Plant. Cell Physiol.*, **48**, 1450–1461.
38. Aotani, D., Ebihara, K., Sawamoto, N., Kusakabe, T., Aizawa-Abe, M., Kataoka, S., Sakai, T., Iogawa, H., Ebihara, C., Fujikura, J. *et al.* (2012) Functional magnetic resonance imaging analysis of food-related brain activity in patients with lipodystrophy undergoing leptin replacement therapy. *J. Clin. Endocrinol. Metab.*, **97**, 3663–3671.

厚生労働科学研究費補助金（創薬基盤推進研究事業）
新規創薬を目指した生活習慣病・難治性疾患モデル遺伝子変異ラットの開発と解析
平成２６年度　研究報告書

発行者　厚生労働科学研究費補助金（創薬基盤推進研究事業）
新規創薬を目指した生活習慣病・難治性疾患モデル遺伝子変異ラットの開発と解析
研究代表者　　中尾　一和

連絡先：〒606-8507　京都市左京区聖護院川原町
京都大学大学院医学研究科
メディカルイノベーションセンター
TEL：075-366-7450